Adv Polym Sci (2008) 220: 65–121
DOI 10.1007/12_2008_145

Published online: 28 June 2008

Self-Assembled Polysaccharide Nanotubes Generated from β-1,3-Glucan Polysaccharides

Munenori Numata[1] (✉) · Seiji Shinkai[2]

[1]Department of Bioscience and Biotechnology, Faculty of Science and Engineering, Ritsumeikan University, Kusatsu, Shiga 525-8577, Japan
numata@fc.ritsumei.ac.jp

[2]Department of Chemistry and Biochemistry, Graduate School of Engineering, Kyushu University, Fukuoka 819-0395, Japan

Abstract β-1,3-Glucans act as unique natural nanotubes, the features of which are greatly different from other natural or synthetic helical polymers. The origin mostly stems from

their strong helix-forming nature and reversible interconversion between single-strand random coil and triple-strand helix. During this interconversion process, they can accept functional polymers, molecular assemblies and nanoparticles in an induced-fit manner to create water-soluble one-dimensional nanocomposites, where individual conjugated polymers or molecular assemblies can be incorporated into the one-dimensional hollow constructed by the helical superstructure of β-1,3-glucans. The advantageous point of the β-1,3-glucan hosting system is that the selective modification of β-1,3-glucans leads to the creation of various functional one-dimensional nanocomposites in a supramolecular manner, being applicable toward fundamental nanomaterials such as sensors or circuits. Furthermore, the composites with functional surfaces can act as one-dimensional building blocks toward further hierarchical self-assemblies, leading to the creation of two- or three-dimensional nanoarchitectures.

Keywords Helical structure · Inclusion complex · Nanomaterials · Polysaccharide · Self-assemble

Abbreviations

AFM	Atomic force microscopy
ANS	1-Anilinonaphthalene-8-sulfonate
CD	Circular dichroism
CD	Cyclodextrins
CLSM	Confocal laser scanning microscopy
CMA	Carboxymethylated amylose
CUR	Curdlan
DPB	1,4-Diphenylbutadiyne
DMSO	Dimethyl sulfoxide
EDS	Energy dispersive X-ray spectroscopy
FITC	Fluorescein isothiocyanate
ICD	Induced circular dichroism
MA	2,3-*O*-Methylated amylose
ORD	Optical rotatory dispersion
PANI	Poly(aniline)
PEDOT	Poly(3,4-ethylenedioxythiophene)
PMDS	Permethyldecasilane
Poly(C)	Polycytidylic acid
PPE	Poly(*p*-phenylene ethynylene)
PT	Poly(thiophene)
PS	Poly(silane)
SEM	Scanning electron microscopy
SPG	Schizophyllan
SWNT	Single-walled carbon nanotubes
TEM	Transmission electron microscopy
TMPS	Trimethoxypropylsilane
TNS	2-*p*-Toluidylnaphthalene-6-sulfonate
VIS-NIR	Visible-near-infrared

1 Introduction

1.1 Polysaccharide Nanotubes

Polysaccharides are abundant organic compounds in nature, constituting a significant portion of our diet, and serve mainly as energy stores, e.g., starch in plants and glycogen in animals. With regard to potential pharmaceutical effects of polysaccharides, they capture intense attention as "biomaterials". Besides, the inherent bio-degradable nature of polysaccharides makes them potential candidates for "eco-materials", such as green-plastics. The peculiar physical and chemical properties of polysaccharides certainly play a significant role in animals and plant cells. For example, some polysaccharides possess inherently stiff and rigid structures, which cause mechanical strength, like cellulose in plants, peptidoglycans in bacteria and chitin in the exoskeletons of arthropods. Furthermore, specific saccharide chains serve as cell surface recognition signals for antibodies, hormones, toxins, acting as indispensable biopolymers for our life through strict molecular recognition.

Nature produces numerous kinds of polysaccharides in an appropriate biological environment. The structural diversity of the natural polysaccharide is fully commensurate with a diverse array of molecules that can be generated from only a limited number of monosaccharides as building blocks by linking them in a variety of ways. This structural feature of polysaccharide characterized by diversity is in sharp contrast to that of other natural polymers such as polynucleotides and peptides with very regular, uniform and well-identified nanostructures.

Recently, the greatest growth has been achieved in the structured determination of natural polysaccharides, and hence this has increased our understanding in relation to structural features as well as functionalities of polysaccharides [1]. The basic knowledge of the structural feature of polysaccharides is essential toward the application as fundamental nanomaterials. For example, X-ray diffraction patterns of various natural polysaccharides have revealed that some of them adopt well-defined helical nanoarchitectures such as polynucleotides, which have never been produced through an artificial polymerization reaction, encouraging us to pursue the possibilities of natural nanotubes.

1.1.1 Amylose

Amylose is a most familiar polysaccharide with regular helical structures defined at the nanoscale (Fig. 1). Carbohydrates are stored in the starch form,

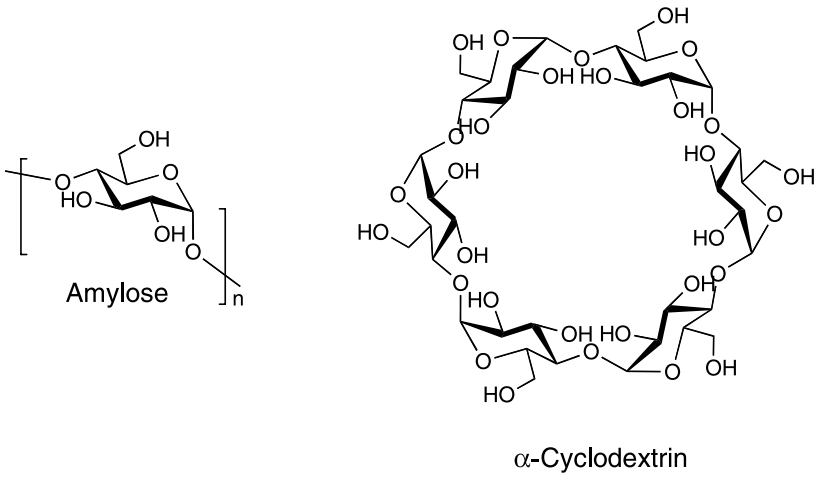

Fig. 1 Repeating units of amylose and α-cyclodextrin

which is a mixture of amylose and amylopectin. Amylopectin is a branched polymer, whereas amylose is essentially a linear polymer of (1 → 4) linked α-D-glucose units, i.e., the unbranched portion of starch. Natural amylose exists as a double-stranded parallel helix, involving two main polymorphs, whereas a single-stranded amylose can be seen in DMSO (Fig. 2). These amylose polymorphs commonly take the same helical parameters, i.e., diameter of 1.3 nm and pitch of 0.8 nm involving six glucose residues per turn [2–4]. This structural feature of amylose can be regarded as one of the typical helical nanotubes, and actually amylose forms the well-known "blue complex" with iodine [5, 6]. In addition, various low molecular organic molecules, such as DMSO, *n*-butanol and *n*-pentanol are also entrapped in the amylose helical cavity [7–10]. The main driving force for the guest binding is hydrophobic interaction that occurs only in the hydrophobic amylose cavity. On the basis of these fundamental investigations on the potential hosting ability of amylose, so far, several research groups have independently demonstrated that amylose can entrap various functional molecules or polymers, leading to the creation of one-dimensional supramolecular complexes. For example, Kim et al. have reported that hydrophobic cyanine dyes with alkyl tails are entrapped into the helical cavity to give water-soluble complexes [11, 12]. The hydrophobic nature in the dye molecules with long alkyl tails is indispensable for the formation of the stable inclusion complexes. The inclusion of the highly polarized dye molecules is of interest in the light of materials science. For example, the supramolecular dye assemblies created with the assistance of the amylose host show unusual thermochromic or optical behaviors, such as second-harmonic generation effects. Once guest dye molecules are entrapped into the cavity, stretching out along the helix axis, the conformational

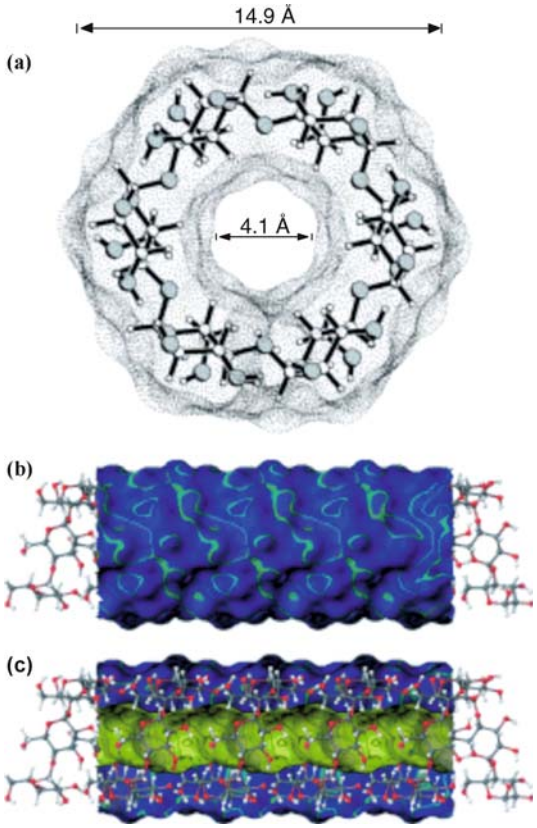

Fig. 2 Example of crystallographic conformation of V_H-amylose. (**a**) Hydrophilic outer surface and (**b**) Inner hydrophobic cavity in *yellow* (**c**). Reprinted with permission from [5]

freedom of dye molecules drastically decreases owing to host–guest interactions, resulting in enhanced fluorescence intensity or unusual thermochromic behavior.

Oligosilanes are σ-conjugated conducting polymers, possessing unique electronic properties due to their electron delocalization along the main chain. Sanji and Tanaka reported that partially carboxymethylated amylose (CMA) can entrap the oligosilane in the helical cavity to give insulated wire-like architectures [13, 14]. The chemical treatment of natural amylose weakens the intra- or interpolymer hydrogen-bonding interactions, so that amylose assumes a somewhat flexible conformation, accompanied with improvement of water-solubility. The powder X-ray diffraction studies revealed that CMA adopts an 8_1-helical structure after incorporation of oligosilane, indicating that the cavity of CMA is somewhat enlarged by the guest inclusion. From CD spectroscopic studies of the complex, the incorporated oligosi-

lane adopts the helical conformation influenced by the chiral cavity of CMA, forming a diastereomeric complex. Similar phenomena are also observed for oligothiophene/CMA systems, that is, oligothiophenes are insulated into the chiral CMA cavity which forces the oligothiophene to adopt a helical conformation [15].

Akashi et al. have demonstrated that chemically modified amylose, i.e., partially 2,3-*O*-methylated amylose (MA), also exhibits excellent hosting ability toward polymer guests such as poly(tetrahydrofuran) and poly(ε-caprolacton) [16]. The helix content of MAs, which is regarded as a measure of the helix-forming ability, could be tuned by the methylation ratio. They investigated the potential abilities to form nanotubes for a series of MAs with different methylation ratios. Consequently, MAs with a moderate methylation ratio tend to form stable inclusion complexes with the selected guest polymers, suggesting the view that these MAs contain some continuous helical segments that play an essential role for improving the inclusion ability of amylose toward guest polymers.

An alternative strategy toward the formation of such inclusion complexes, reported by Kadokawa et al., is to use the enzymatic polymerization of glucose on a template polymer, where phosphorylase catalyzes a polymerization reaction of α-D-glucose 1-phosphate monomer along the template polymer [poly(tetrahydrofuran)] in a twisting manner [17]. The same inclusion complex was not formed upon just mixing natural amylose with polymer [poly(tetrahydrofuran)], probably due to the rigid conformation of natural amylose.

In view of the creation of functional inclusion complexes, single-walled carbon nanotubes (SWNTs) would be an ultimate target polymer due to their potential as fundamental nanomaterials. Aiming at the practical application of SWNTs as functional polymers, the difficult handling arising from their poor solubility and strong cohesive nature is a serious problem for chemists. Accordingly, formation of the inclusion complex with SWNTs would be a new path to accelerate development of carbon nanotube chemistry. The first example is SWNT/amylose composite formation reported independently by Kim et al. and by Stoddard et al. [18, 19]. It was shown therein that SWNTs can be incorporated into the amylose cavity to form stable inclusion complexes. Considering the diameter of SWNTs (1–2 nm), the cavity size of natural amylose (ca. 0.4 nm) would be changed by the inclusion of SWNTs.

Natural amylose and its chemically modified form, i.e., CMAs and MAs, possess basically a rigid cavity, and therefore, they can include guest molecules or polymers in a size-selective manner because the cavity can act flexibly in an induced-fit manner, being different from those of cyclodextrines (CDs). From the stand point of the nanotube structure, this is in contrast to CD hosts in rigidity and ring structures.

1.1.2 Cyclodextrin Arrays

Cyclodextrins (CDs) are cyclic compounds consisting of six to eight glucose units; i.e., α-, β- and γ-CDs (Fig. 1). The cavity sizes of these CDs are 0.43 nm, 0.60 nm, and 0.74 nm, respectively [20]. These cyclic cavities are constructed with $\alpha(1 \rightarrow 4)$-linked glucose units in the same fashion as for the amylose cavity. Once the polymeric guest threads through the CD cavities, CDs are assembled into array structures, which are now called pseudo-polyrotaxane structures. One may regard them as a sort of self-assembled carbohydrate nanotube [21–23]. Therefore, we herein overview CD arrays as a potential self-assembled nanotube, characterizing the difference between CDs and β-1,3-glucan hosting systems.

CDs are known to form inclusion complexes with various low-molecular weight compounds, including nonpolar aliphatic molecules, polar amines and acids as well as various polymers [24]. Along this line, CDs also have ideal structures for the construction of molecular nanotubes [25–28]. Harada et al. have successfully demonstrated that a series of CDs are threaded onto a polymer chain to give pseudo-polyrotaxane structures [29–34]. For example, α-CDs form a polyrotaxane structure with poly(ethylene glycol), which is obtained as a crystalline precipitate. The powder X-ray diffraction pattern of the precipitate led to the conclusion that α-CDs are tightly packed on the polymer in a head-to-head manner. It is worth mentioning that β-CDs and γ-CDs also exhibit similar hosting abilities as α-CDs, the size correlation between their cavity size and the diameter of guest polymers being well recognized: β-CDs form complexes not with poly(ethylene glycol) but with poly(propylene glycol), which is slightly larger than poly(ethylene glycol) in its diameter. Similarly, γ-CDs form complexes with poly(methyl vinyl ether), whereas α-CDs and β-CDs do not give complexes with this polymer. Strictly speaking, however, these polyrotaxanes may not be "true" nanotubes because CD units are not connected by covalent bonds. Interestingly, the cross-linking of the adjacent CDs on a template polymer leads to the creation of complete tubular structures even after removing the template, where temporarily formed tubular structures are fixed on the template polymer through the chemical treatment.

After the initial research on CD nanotubes by Harada et al. and by Wenz et al. the intriguing systems have been widely extended to various functional polymers such as conjugated polymers (Fig. 3d), including poly(aniline) (PANI), poly(thiophene) (PT), poly(silane) (PS), etc., which can also thread through the CD cavities to form the polyrotaxane-type complexes (Fig. 3b) [35–50]. In view of the fundamental research on the conjugated polymers, the advantageous point of the CD nanotube systems is that the functional polymers can be well insulated as an individual polymer chain even in their solution and in the solid state. Since the conjugated polymers

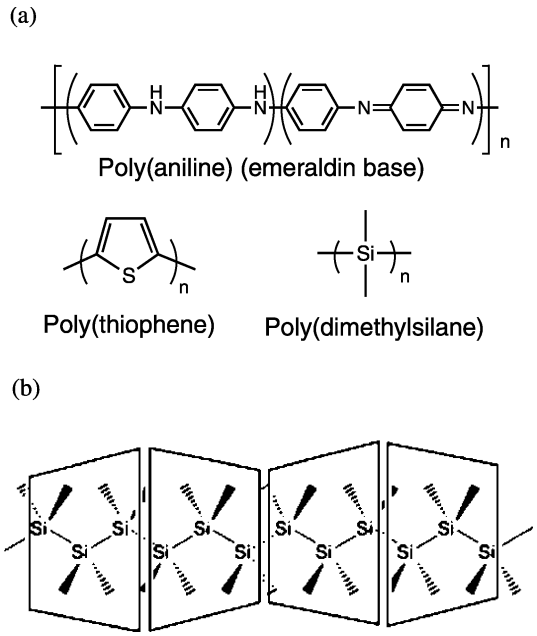

Fig. 3 Example of π- and σ-conjugated polymer guests threading into the CD cavity (*top*) and example of self-assembled γ-CD nanotube including poly(dimethylsilane). Reprinted with permission from [49]

have a strong tendency to form an insoluble aggregate mass mainly due to their strong stacking nature, the insulated polymer would provide dramatic advantages in relation to the stability as well as the electronic and photochemical properties of the guest polymers.

1.2 β-1,3-Glucans

1.2.1 Structural Aspects of β-1,3-Glucans

β-1,3-Glucans are present in a number of fungi, where they function as a structural polysaccharide like cellulose, e.g., extracellular microbial polysaccharide and they are essentially a linear polymer of (1 $\rightarrow$ 3)-linked β-D-glucose units (Fig. 4) [51–65]. Among a series of β-1,3-glucans, curdlan (CUR) is known as one of the simplest β-1,3-glucans [60–65]. X-ray diffraction patterns of CUR in the anhydrous form revealed that it adopts a right-handed 6_1 triple helix with a diameter of 2.3 nm and pitch of 1.8 nm (Fig. 5) [61, 65]. In contrast to the simple CUR structure, SPG has side glucose groups linked at every third main-chain glucose. The side glucose groups

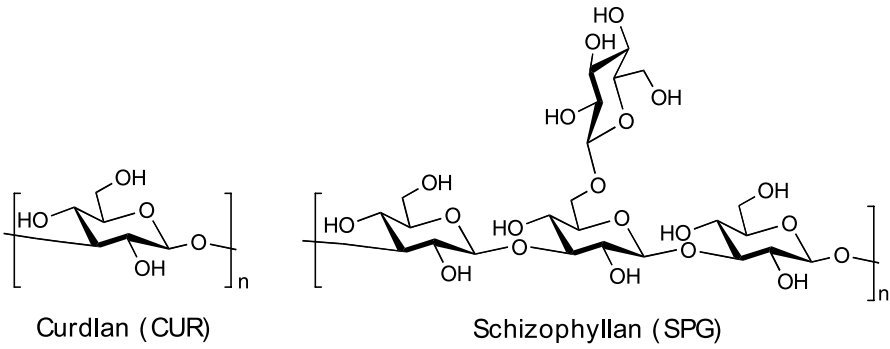

Fig. 4 Repeating units of β-1,3-glucans: CUR and SPG

endow SPG with water solubility, whereas they do not affect the helical conformation of the main chain. The helical parameters of β-1,3-glucans are almost consistent with those of double-stranded DNA, but somewhat larger than those of amylose, indicating that CUR adopts a wide helical structure. Atkins et al. have revealed by X-ray diffraction patterns that in the triple helix structure of CUR, three glucoses composed of different chains are bound together through the hydrogen bonds among the three O-2 atoms, forming the one-dimensional hydrogen-bonding network in the triple helix [64]. This structural analysis revealed that in the triple helix there is not enough space to accommodate even small molecular guests. Therefore, the sole strategy for β-1,3-glucans to exert their hosting ability is to dissociate the original triple helix into a single strand, losing the inner hydrogen-bonding network: these dissociated β-1,3-glucan chains would possess potential ability to include guests and to form nanotubes.

Norisuye et al. have reported the interesting solution properties of β-1,3-glucans where denaturing and renaturing of the triple helix can take place reversibly; that is, schizophyllan (SPG) dissolve in water as a triple helix (t-SPG), whereas as a single chain in DMSO (s-SPG). When water is added to the DMSO solution, however, renaturing of s-SPG is promoted, resulting in the formation of the original triple helix (Fig. 5d) [51, 59, 61, 66, 67]. CUR with an appropriate molecular weight also exhibits a similar reconstructing ability of the triple helix.

1.2.2 Complexation Between β-1,3-Glucans and Polynucleotide

Recently, Sakurai et al. reported the first example of β-1,3-glucan forming a macromolecular complex with some polynucleotides; that is, when the renaturing of β-1,3-glucan was carried out in the presence of some polynucleotides, it formed novel triple-stranded structures consisting of two β-1,3-

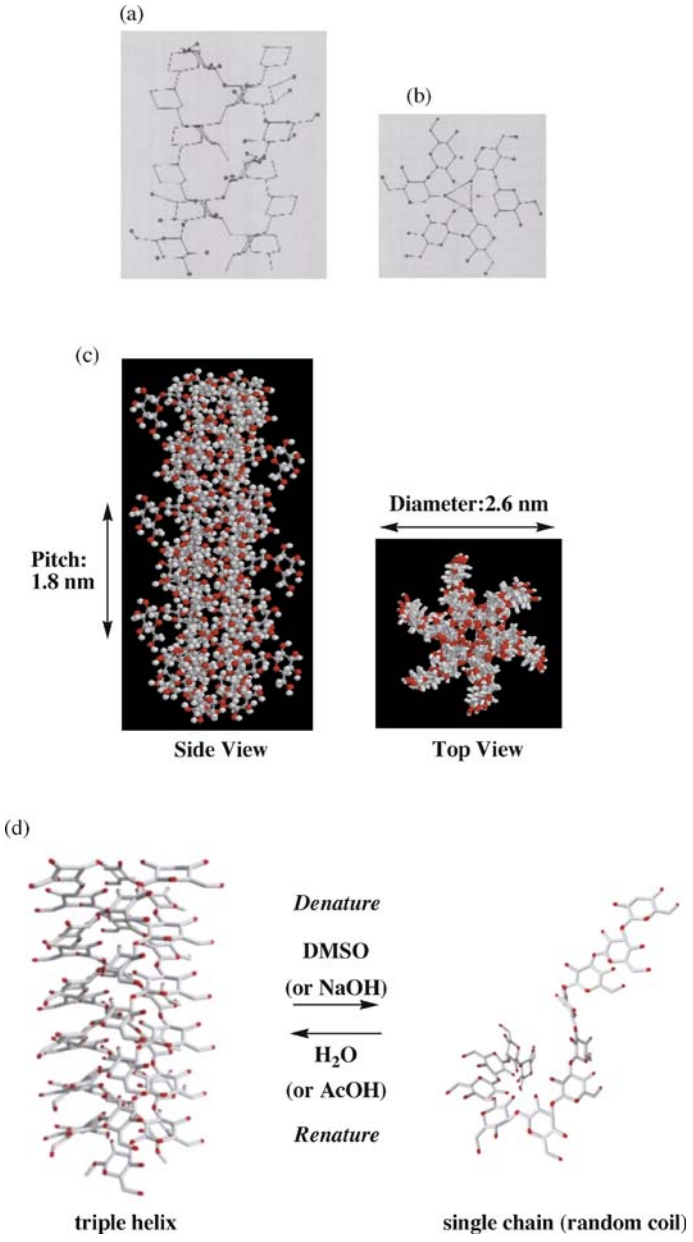

Fig. 5 Projection of the CUR triple helix **a** in the *x*–*z* plane and **b** in the *x*–*y* plane, showing the hydrogen-bonding network constructed in the helix (hydrogen atoms are omitted for both structures) (Reprinted with permission from [64]). **c** Calculated SPG triple helix structures based on the crystal structure of CUR and **d** Schematic illustration of denature/renature processes

glucan chains and one polynucleotide chain [68, 69]. These findings imply that β-1,3-glucan can interact with guest polymers only in its dissociated state, which would allow the glucose main-chain to adopt various conformations different from the original triple helix. The main driving force for the formation of the macromolecular complexes is considered to be hydrophobic interaction in addition to hydrogen-bonding interactions occurring inside the novel triple helix. These intriguing findings encouraged us to apply this unique and unusual hosting system to other functional polymeric guests, where the denaturing and renaturing processes play a significant role in inclusion of various functional materials, such as polymers, molecular assemblies, inorganic particles, etc.

2
Unique One-Dimensional Hosting Abilities

2.1
Inclusion of Single-Walled Carbon Nanotube (SWNT)

Since the discovery of single-walled carbon nanotubes (SWNTs) by Iijima, they have been regarded as ideal nanomaterials due to their unique electronic, photochemical, and mechanical properties [70–72]. Much effort has been paid to apply SWNTs as practical nanomaterials, however the strong cohesive nature and poor solubility of SWNTs have caused a serious problem; that is, these properties hamper work on SWNTs as "functional polymers". As a potential solution to this problem, it would be worth wrapping SWNTs with synthetic or biological polymers, promoting dissociation of the SWNT bundle to give a homogeneous solution without damaging SWNT surfaces [73–79]. In particular, a natural polysaccharide such as amylose is an excellent solubilizer for SWNTs, because polysaccharides have no light absorption in the UV-VIS wavelength region, which is suitable for exploiting the photochemical properties of the resultant composite.

The main driving forces for the reconstruction of the triple-stranded β-1,3-glucans from the single-stranded ones are considered to be the hydrophobic interaction in addition to the hydrogen-bonding interactions. On the basis of this experimental fact, it is expected that SWNTs might be entrapped in the inside hollow of the β-1,3-glucans helical structure mainly owing to the hydrophobic interaction (Fig. 6). Unlike the amylose hosting system, however, natural β-1,3-glucans do not have enough cavity to accommodate SWNT with 1–2 nm diameters. Thus, some conformational change in the β-1,3-glucan main-chain would be needed after entrapping the guest polymers.

As a preliminary experiment to investigate whether β-1,3-glucans can actually entrap such a rigid polymer into their cavities, SWNTs were cut into an appropriate length (1–2 μm) by acid treatment, which makes handling of

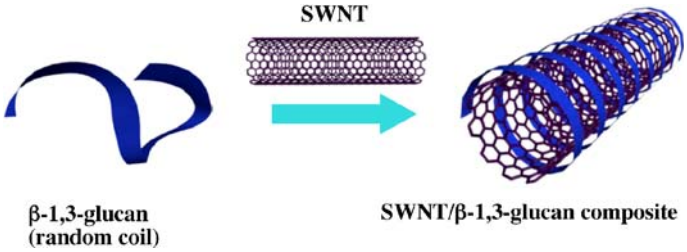

Fig. 6 Schematic illustration of the formation of SWNTs/β-1,3-glucan composite

SWNTs easy [80–83]. As a result, the cut SWNTs (c-SWNTs) can be easily dispersed into water, but they still tend to form bundle structures several tens of nanometers in diameter. Consequently, an s-SPG (M_w = 150 kDa) DMSO solution was directly added to an aqueous solution containing the bundle c-SWNTs, according to the same procedure as for the polynucleotide guests, expecting that SWNTs are entrapped into the SPG cavity [68]. To remove an excess amount of SPG feed, the resultant solution was subjected to centrifugations. The presence of c-SWNT in the obtained aqueous solution was evidenced by the measurements of VIS-NIR and Raman spectroscopy. The direct evidence that SWNTs are really entrapped into the SPG cavity was obtained by Atomic Force Microscopy (AFM). Interesting, when c-SWNTs were dispersed with the aid of SPG into water, the surface of the fibrils showed a periodical structure with inclined stripes, reflecting the strong helix-forming nature of the β-1,3-glucan main-chain (Figs. 7 and 8). Subsequently, the periodical interval in the helical stripes was estimated by AFM. It was confirmed from scanning along a fibril that the mountain and the valley appear periodically at 16 nm intervals. In addition, from the height profile analysis by AFM, it was revealed that most composites are ca. 10 nm in height, indicating that β-1,3-glucans can wrap around bundle c-SWNTs, with a change in their original helix parameters. As a reference experiment, on the other

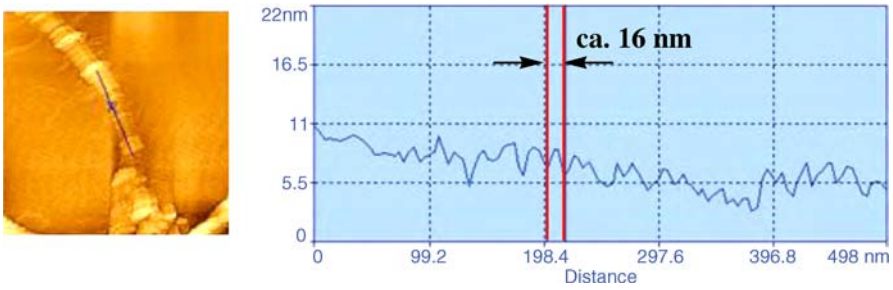

Fig. 7 AFM image of c-SWNTs bundle/SPG composite and its scanning profiles of vertical section plans. Reprinted with permission from [86]

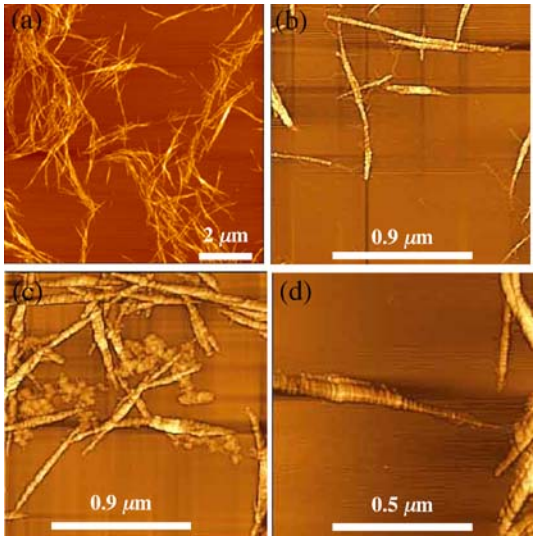

Fig. 8 AFM images of **a** c-SWNTs, **b** c-SWNTs/SPG composite, **c** c-SWNTs/CUR composite, **d** Magnified picture of fibrils in s-SWNTs/SPG composite. Amorphous structure observed around the composite is considered to be uncomplexed CUR which cannot be removed during centrifugation process due to its poor solubility in water

hand, when a DMSO solution of s-SPG was cast on mica, we could observe a fine polymeric network structure. Besides, the surface of c-SWNTs themselves did not give any specific patterns as seen in the composite surface. These results clearly show that β-1-3-glucan can act as a one-dimensional host for SWNTs, where the characteristic helical structure of β-1-3-glucans is reconstructed on the SWNTs surface [84]. The β-1,3-glucan one-dimensional host is characterized by this well-identified wrapping mode arising from the strong helix-forming nature of β-1,3-glucans; that is, the hydrophobic inner surface of β-1,3-glucans interact with SWNTs, whereas a hydrophilic surface exists on the composite surface. It should be noted that only the composites containing bundle SWNTs are intentionally highlighted for microscopic observation because the helical structure constructed on such a composite can be easily recognized by microscopic techniques.

Natural CUR is scarcely soluble in water due to the lack of side glucoses. Nevertheless, when a CUR chain was cut into a moderate length, e.g., several tens of thousand, by formic acid-hydrolyzed treatment [85], the resultant CUR acts as a one-dimensional host like SPG. Actually, when s-CUR was used as a wrapping agent instead of s-SPG, a similar periodical structure as seen in the c-SWNT/SPG composite can be observed on bundled SWNTs (Fig. 8c) [84]. The findings lead to the conclusion that the $\beta(1\rightarrow3)$ glucose linkages are indispensable for the unique hosting capabilities of β-1,3-glucans.

The novel SWNTs/β-1,3-glucan composites thus obtained were thoroughly characterized by several spectroscopic and microscopic methods including HRTEM, EDS-TEM, SEM, CLSM, which consistently support the view that the β-1,3-glucans really wrap SWNTs.

SWNTs exhibit their unique electronic and photonic properties only when they exist as an individual fiber. Taking the fact that SPG and CUR adopt the tight helical structure in their natural state, they are expected to wrap one-piece of SWNTs into their hydrophobic cavity, avoiding the formation of the unfavorable bundle structure. Here, if we intend to apply the resultant composite to practical nanomaterials, as-grown SWNTs (ag-SWNTs) are favorable because of no electrochemical defect on the SWNT surface. Although, unlike c-SWNTs, ag-SWNTs have a strong tendency to form the bundle structure, they are easily dispersed into water after entrapping into the β-1,3-glucan cavity with the aid of sonication. This remarkable solubilization capability even for ag-SWNTs allows us to investigate the detailed properties of the resultant composites [86]. First, the ag-SWNTs/SPG composite was subjected to VIS-NIR measurements in D_2O solvent (Fig. 9). The characteristic sharp bands assignable to individual SWNTs can be observed in the VIS-NIR region, supporting the view that one or a few pieces of ag-SWNTs are included in the SPG helical structure. AFM observations support the view more quantitatively. From the height profile of the composite, it can be recognized that most of them are 2–3 nm in diameter and the distribution is very narrow. Furthermore, when the surface of the composite was scanned along the fibril, a periodical pattern as seen in the c-SWNT/SPG

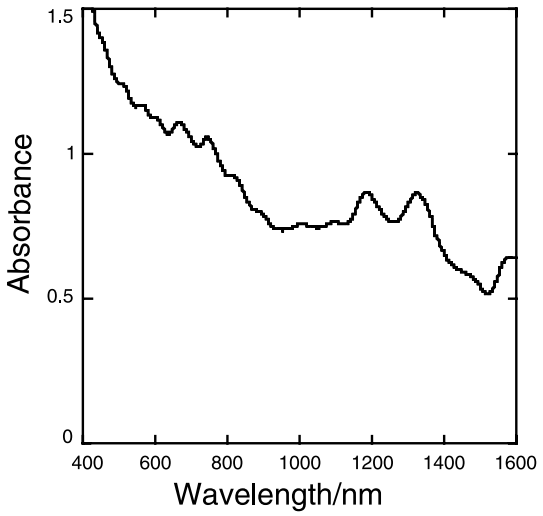

Fig. 9 VIS-NIR spectrum of ag-SWNTs/SPG solution: D_2O, cell length 1.0 cm , room temperature. Reprinted with permission from [86]

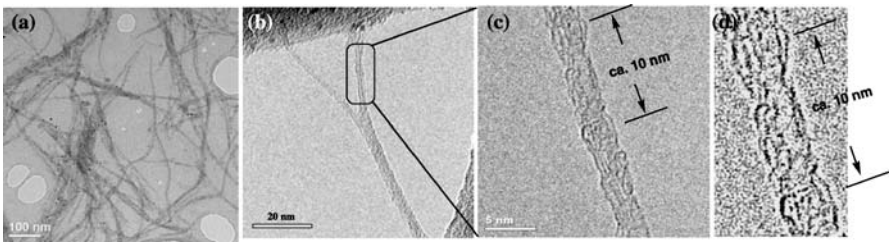

Fig. 10 **a** TEM image of ag-SWNT/SPG composite, and **b**, **c** its magnified picture. **d** The original image of (**c**) was Fourier filtered to enhance the contrast of the composite. Reprinted with permission from [86]

composite can be recognized. Subsequently, the ag-SWNTs/SPG composite was directly characterized by high-resolution TEM (HRTEM). From Fig. 10, the composites are visually recognized to be a very small, fibrous structure but not a bundled structure. Moreover, clearly recognized in the Fourier filtered image was that two s-SPG chains twine around one ag-SWNT, providing "decisive" evidence that one piece of ag-SWNTs is wrapped by s-SPG chains. The helical pitch is estimated to be ca. 10 nm, which is longer than that of the original triple helix, suggesting the view that the conformation of SPG chains is changeable with incorporation of guests, in sharp contrast to CDs or amylose systems. These conformational changes in the main-chain would be allowed only for the single- or double-stranded helix and therefore the denaturation process of the original triple helix should be indispensable for the guest inclusion. Recently, Coleman and Ferreira presented a simple and general model that describes the ordered assembly of polymer strands on nanotube surfaces, the energetically favorable coiling angles being estimated to be 48–70° [87]. This theoretical approach is partly complementary to our present results, but their single chain wrapping system cannot be directly compared with our two-chain wrapping system.

Today, electron tomography is expected to play a central role in characterization of composite nanomaterials, because it can provide a real three-dimensional distribution map of constituent materials [88–93]. This imaging technique was applied to our composite nanomaterials consisting of two nanofibers. The three-dimensional structures are reconstructed from an angular series of two-dimensional structure in Fig. 10b. The four selected stills are shown in Fig. 11, where ag-SWNT appears as a white fine fibril (for example, the right branch in the 45° rotating image) and the SPG thin layer wraps the fibril. The s-SPG chains exist as a uniform layer around one or two pieces of ag-SWNTs even viewing from any angle. This fact implies that s-SPG *wraps* one piece of ag-SWNT.

If β-1,3-glucans maintain their characteristic helix-forming nature even on the SWNT surface, the dissociation from SWNTs would be promoted by add-

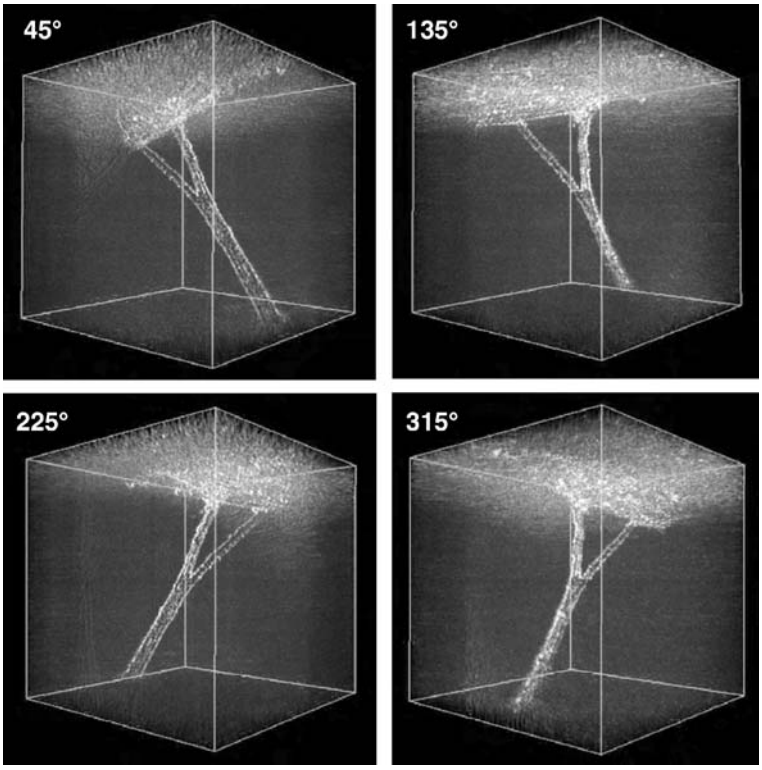

Fig. 11 Reconstructed three-dimensional images of ag-SWNTs/SPG composite, viewed from different orientations. These correspond to the clockwise rotation images of the two-dimensional image in Fig. 10b, rotating around a perpendicular axis with 45, 135, 225 and 315°, respectively. Reprinted with permission from [86]

ition of DMSO or NaOH, in which β-1,3-glucans exist as a single chain. As shown in Fig. 12, when DMSO was added to the aqueous solution containing the composite adjusting the final composition to be 50% v/v, the entrapped ag-SWNTs were immediately precipitated out. This result gives the strong impression that the composites are stabilized by noncovalent interactions occurring between the hydrophobic core and the hydrophilic shell, which can be easily peeled off by the various chemical stimuli.

As a summary of the forgoing findings, particularly interesting are the facts that (1) the periodical stripe structure, which stems from a helical wrapping mode characteristic of β-1,3-glucans, is confirmed, and (2) β-1,3-glucans have potential abilities to accommodate various guest polymers due to their flexible conformational changes, without being affected by the diameter as well as the chemical properties of guest polymers.

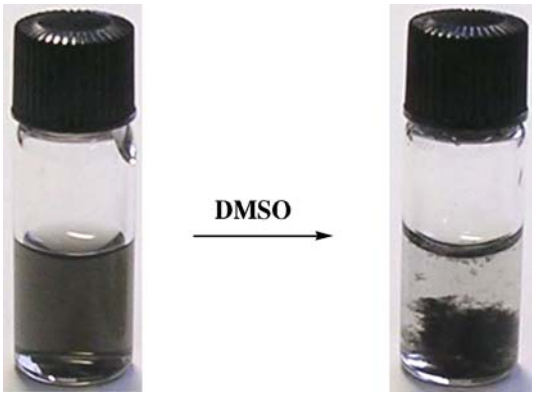

Fig. 12 Picture of aqueous ag-SWNTs/SPG composite solution (*left*) and that taken after addition of DMSO (*right*): The final solution contains 50% v/v DMSO. Addition of aqueous 1.0 M NaOH solution results in a similar precipitation of ag-SWNTs. Reprinted with permission from [86]

2.2 Inclusion of Conjugated Polymers

2.2.1 Inclusion of Poly(aniline) (PANI)

PANI is one of the most promising and widely studied conductive polymers owing to its high chemical stability, high conductivity, and unique redox properties [94–96]. In spite of these advantages, PANI and its derivatives are hardly applicable for conductive nanowires in a bottom-up manner, because these PANIs tend to form amorphous aggregates composed of highly entangled polymeric strands. Much research effort has therefore been put into the manipulation of an individual PANI nanofiber and in the fabrication of parallel-aligned strands to show excellent conductivity through the nanofibers.

From the forgoing c-SWNTs/SPG composite system, it would be expected that β-1,3-glucans can fabricate PANI nanofiber structures several tens of nanometer in diameter, acting as a one-dimensional host for PANIs bundles. The objective PANIs/SPG nanocomposites can be prepared through gradual dilution of a DMSO solution containing commercially available PANI (emerardine base, M_w = 10 kDa) and s-SPG (M_w = 150 kDa) with water followed by purification through repeated centrifugation [97]. TEM observations showed the formation of fibrous architectures from PANIs/SPG nanocomposites whose lengths were consistent with that of the used SPG (Fig. 13). The observed nanofibers are highly contrasted without any staining due to the adsorption of the electron beam. Importantly, the contrast,

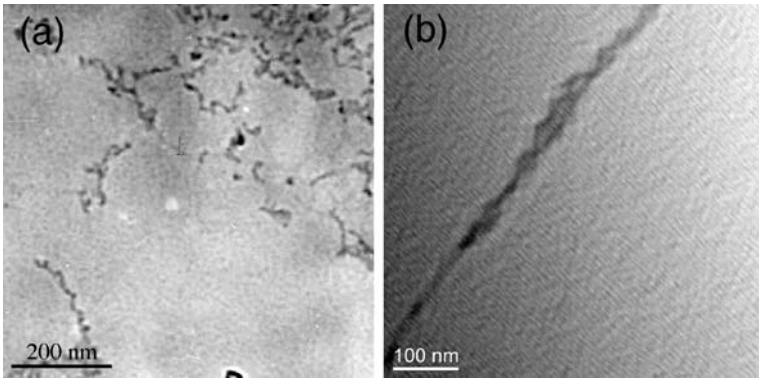

Fig. 13 **a** TEM images of PANIs/SPG composites, **b** Magnified image of (**a**), the images were taken without staining. PANIs themselves afforded spherical massive aggregates. Reprinted with permission from [97]

which should arise from incorporated PANIs, continuously exists all over the range of the obtained composite. Since the length of the used PANIs is rather shorter than that of s-SPG, the incorporated PANIs fibers are bundled into the one-dimensional fibers along the SPG cavity. The diameter of the smallest fiber is estimated to be around 10 nm, indicating that several PANI strands are co-entrapped within the one-dimensional cavity. Amylose is also considered to be a potential host for the creation of such an insulated wire. As far as our investigation, however, amylose could not form such a fine fi-

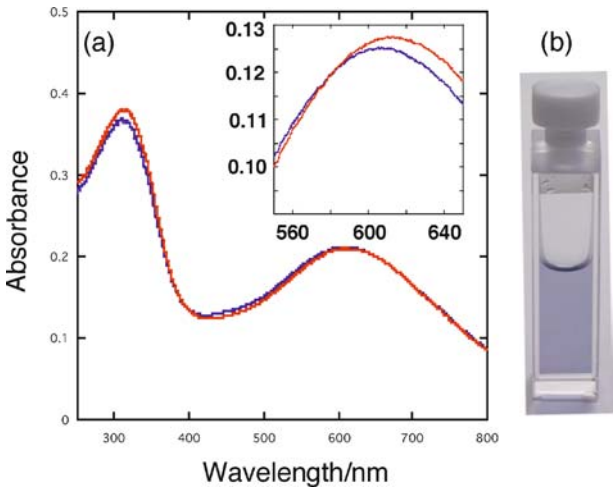

Fig. 14 **a** UV-VIS spectra of PANIs/SPG (*blue line*) and amylose/PANIs (*red line*) aqueous solution, room temperature, cell length 0.5 cm, **b** Photo image of PANIs/SPG aqueous solution. Reprinted with permission from [97]

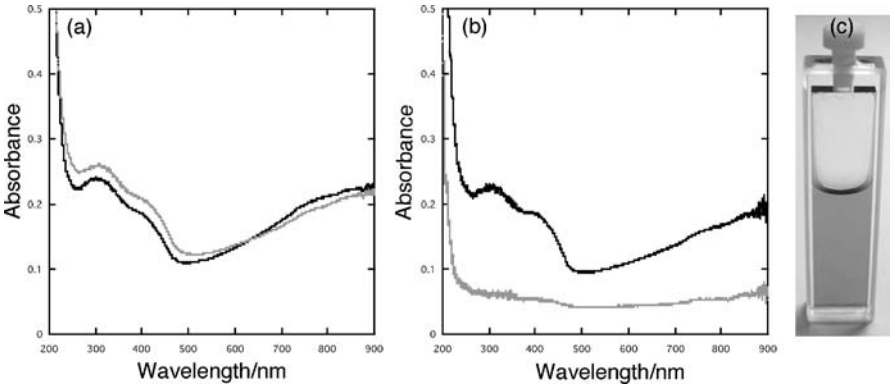

Fig. 15 UV-VIS spectra of **a** PANIs/SPG composite (*black line*) and PANIs/amylose composite (*gray line*) after H^+ doping, **b** After 24 h under the same condition and **c** Photo image of PANIs/SPG composite aqueous solution after doping. Reprinted with permission from [97]

brous structure upon mixing with PANIs according to the same procedure. The PANIs/amylose mixture did not give any significant specific structure in TEM.

Spectroscopic measurements of the composite support the view that PANIs bundles are entrapped into the one-dimensional cavity, which forces PANI fibers to arrange in a parallel fashion, leading to the creation of a nanowire structure (Fig. 14). Furthermore, the obtained PANIs/SPG composite was easily doped by the HCl treatment and the resultant solution was stable for several weeks (Fig. 15). On the other hand, the amylose/PANIs composite formed a precipitate after the same treatment. The morphology of the composite was scarcely changed through this doping process. Taking the fact into account that the diameter of the composite is rather larger than that of native t-SPG, SPG would wrap PANIs bundles in a somewhat disordered conformation, which would allow the dopant to reach the PANIs surface. This system would be useful for fabricating PANI nanofibers in a supramolecular manner.

2.2.2 Inclusion of Poly(thiophene) (PT)

So far, several intriguing approaches have been developed to fabricate an individual PT fiber, including a covalent and noncovalent approach in which the PT backbone is shielded by wrapping within a dendritic wedge or threading PT through CDs sheath [98–102]. Along this line, the composite formation between SPG and PT is of interest as a new approach leading to the creation of novel PT molecular wires [103]. To prepare a well-ordered one-dimensional nanocomposite, the strong π–π stacking interactions among PT backbones

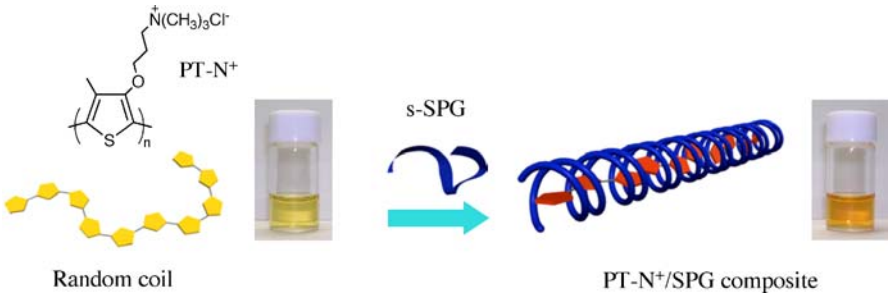

Fig. 16 Schematic illustration of the chirally insulated PT-N^+ in the helical SPG cavity

should be suppressed before being insulated into the β-1,3-glucan cavity. In the present study, water-soluble cationic polythiophene (PT-N^+) was synthesized for the well-identified composite formation, because it would interact with β-1,3-glucan as an individual polymer. Expectedly, the polycationic nature of PT-N^+ and the resultant weakened packing mode would result in a well-characterized PT-N^+/SPG complex, in which only one PT strand is encapsulated within the one-dimensional cavity of SPG (Fig. 16). Figure 17a and b shows absorption and emission spectra, comparing the PT-N^+ and PT-N^+/SPG composites. The absorption maximum of PT-N^+ appears at 403 nm, whereas that of PT-N^+/SPG is drastically red-shifted to 454 nm by ca. 50 nm, demonstrating that SPG forces the PT backbone to adopt a more planar conformation which increases the effective conjugation length. In the general case, when PTs form π-stacked aggregates in poor solvent, the UV-VIS spectrum is characterized by the appearance of a vibronic band in the longer wavelength region [104]. In the present system, however, such a peak attributable to the stacked aggregate was not observed.

The emission maximum (561 nm) of PT-N^+/SPG composites is also red-shifted from that of free PT-N^+ (520 nm) and slightly increases in intensity, supporting the view that the PT-N^+ backbones become more planar and more isolated in the SPG cavity. It should be emphasized that no red shift of the absorption peaks is observed for the cast films of PT-N^+/SPG composite, indicating that the PT-N^+ backbone is shielded by the SPG sheath, by which unfavorable interpolymer stacking of the PT-N^+ backbone is strongly restricted even in the film. In addition, although the SPG sheath surrounds the PT-N^+ backbone, the characteristic wrapping modes, e.g., somewhat elongated helical pitch, would allow small molecules to interact with the PT-N^+ backbone directly, as observed in doping of the PANI/SPG composite. This is in contrast to the sheath of CD arrays, providing a cyclic closed cavity.

The CD spectra of the composites show an intense split-type ICD in the π–π^* transition region (Fig. 17c). This fact clearly suggests that PT-N^+ would be chirally twisted in an intrastranded manner. The observed ICD patterns are characteristic of a right-handed helix of the PT backbones, reflecting the

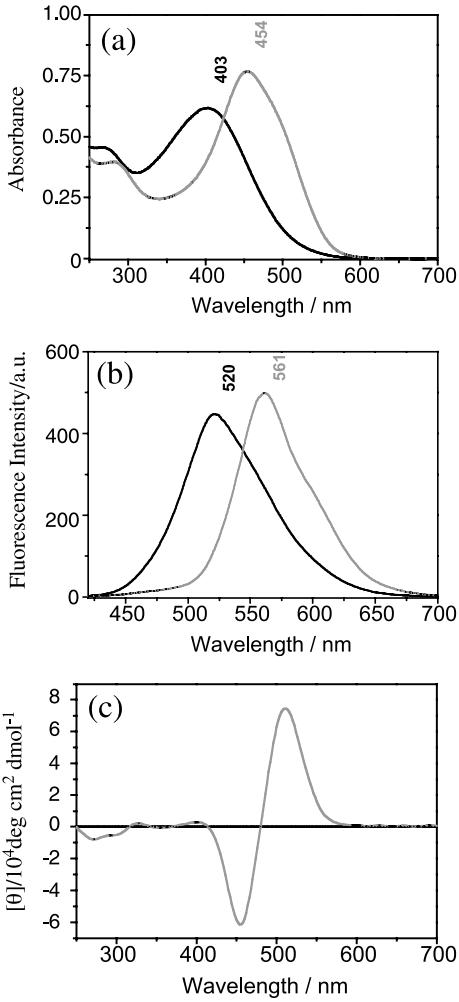

Fig. 17 **a** UV-VIS and **b** Emission (λ_{ex} = 400 nm) spectra of PT-N^+: the spectra were taken without SPG (*black line*) and with SPG (*gray line*)

right-handed helical structure of SPG [105]. The stoichiometry of the complex was determined by means of continuous-variation plots (job plots) from the CD spectra (Fig. 18). Consequently, the molar ratio of glucose residues along the main chain to the repeating unit of PT-N^+ can be determined to be around 2. The complexation mode of the PT-N^+/SPG complex is almost similar to that of the polynucleotide/SPG complex, leading to the conclusion that SPG tends to form hetero-macromolecular complexes by exchanging one glucan chain in t-SPG for one water-soluble guest polymer.

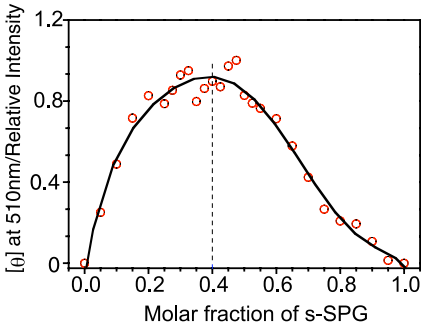

Fig. 18 Job plot obtained from the CD spectra

2.2.3 Inclusion of Poly(*p*-phenyleneethynylene) (PPE)

PPE is a conjugated polymer which can convert chemical and physiological signals into optical emission with signal amplification. Therefore, PPE has been regarded as a conjugated polymer suitable for chemosensors due to its excellent optical response to environmental variation through the relatively free rotation of the alkenyl-aryl single bond [106–113]. A particularly challenging aspect of PPE is to design a water-soluble PPE backbone with a one-handed helical structure because it is readily applicable as a sensitive chiral sensor targeting biologically important molecules and polymers. As a novel approach toward the creation of a chiral insulated PPE wire, β-1,3-glucans should exert their unique hosting abilities [114].

Aiming at the creation of a well-characterized complex, water-soluble PPE (PPE-SO_3^-) was used in the present study. Expectedly, upon mixing of PPE-SO_3^- and s-SPG, a clear solution could be obtained. The resultant solution was characterized by UV-VIS, fluorescence and CD spectroscopies. Figure 19 compares the absorption spectra between PPE-SO_3^- itself and its mixture with s-SPG. The absorption maximum of 442 nm observed in the absence of SPG is attributed to a random-coiled conformation of the PPE backbone. Upon mixing with s-SPG, however, the absorption maximum is red-shifted to 470 nm, indicating that the effective conjugation length of the PPE backbone is increased. The shift clearly shows that the interpolymer interaction between PPE-SO_3^- and s-SPG would force the PPE backbone to adopt a planer and rigid conformation. Furthermore, fluorescence spectra of the PPE-SO_3^-/SPG composite revealed that the emission intensity dramatically increases upon addition of s-SPG (Fig. 20). The finding indicates that the PPE backbones do not aggregate by themselves but become more isolated through the complexation with s-SPG, supporting the view that the PPE backbone is insulated into the one-dimensional SPG cavity.

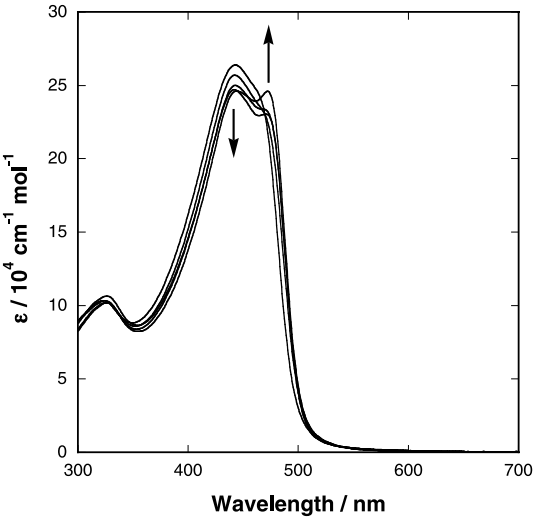

Fig. 19 UV-VIS spectral change of PPE-SO_3^- as a function of SPG concentration (concentration range of s-SPG : $0–6.7 \times 10^{-4}$ M). The concentration of PPE-SO_3^- was kept at 1.5×10^{-4} M. H_2O/DMSO = 95/5 (v/v), 1.0 cm cell length, room temperature. Reprinted with permission from [114]

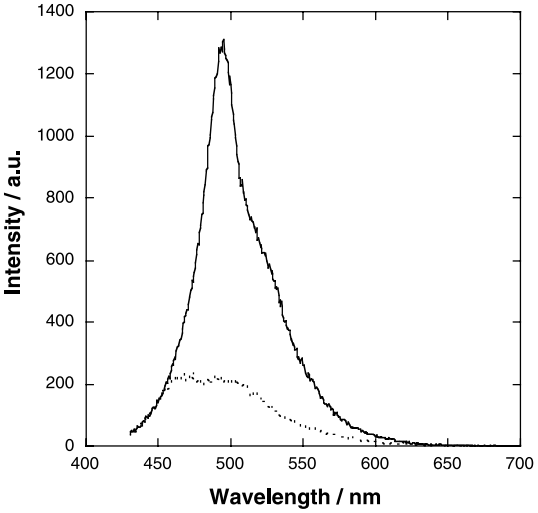

Fig. 20 Emission spectra of PPE-SO_3^- in the absence of s-SPG (*dashed line*) and in the presence of 15.0 eq. (2.3×10^{-3} M) of s-SPG (*solid line*), $\lambda_{ex} = 400$ nm. The concentration of PPE-SO_3^- was kept at 1.5×10^{-4} M. H_2O/DMSO = 95/5 (v/v), room temperature. Reprinted with permission from [114]

CD spectroscopic studies are also helpful to investigate the conformational changes of incorporated PPE-SO_3^-. The shape and ICD pattern of the composite suggest that PPE-SO_3^- would adopt a right-handed helix which is transcribed from SPG to the PPE backbone (Fig. 21). As a reference experiment, we mixed an aqueous solution containing t-SPG with PPE-SO_3^-. However, the mixture did not give any CD signal around the same wavelength region. This result supports the view that the renaturating process from s-SPG is indispensable for the effective interaction between SPG and PPE-SO_3^-. The spectroscopic results above mentioned lead to the conclusion that PPE-SO_3^- is incorporated into the one-dimensional SPG cavity as an individual polymer and its backbone adopts a right-handed twisted conformation along the SPG polymer chain. These results are almost consistent with those observed for the PT-N^+/SPG system, encouraging us to pursue the fundamental properties of SPG as a one-dimensional host.

To elucidate the mechanism for PPE-SO_3^-/SPG complex formation, the stoichiometry of the complex was determined by means of a continuous-variation plot (Job plot) from its CD spectroscopic change. From the Job plot, the maximum complex formation is attained at around 2, which corresponds to the molar ratio of the glucose residue along the s-SPG main chain to the repeating unit of PPE-SO_3^-. Furthermore, considering the facts that t-SPG forms a right-handed 6_1 triple helix with a 1.8 nm pitch and that three *p*-phenylene ethynylene units have statistically 1.6 nm length in average, we suppose that the PPE-SO_3^-/SPG complex prepared from a mixture of s-SPG and PPE-SO_3^-

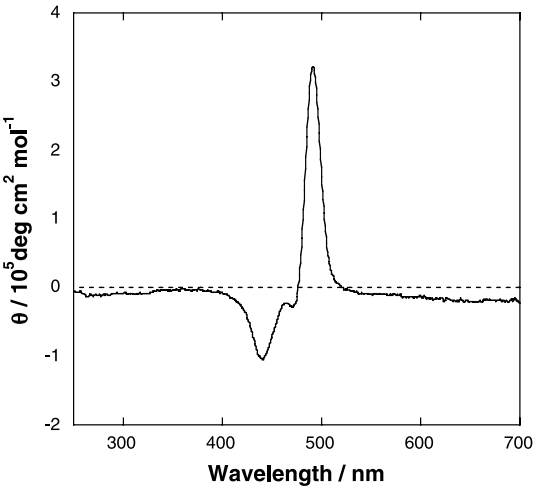

Fig. 21 CD spectra of PPE-SO_3^- in the absence of 15.0 eq. (2.3×10^{-3} M) of s-SPG (*dashed line*) and in the presence of PPE-SO_3^- (*solid line*). The concentration of PPE-SO_3^- was kept at 1.5×10^{-4} M. H_2O/DMSO = 95/5 (v/v), 1.0 cm cell length, room temperature. Reprinted with permission from [114]

is constructed by two s-SPG chains and one PPE-SO_3^- chain in which the two s-SPG chains force the PPE-SO_3^- chain to be twisted. Together with the results obtained from polynucleotide/SPG and PT/SPG complexes, it can be concluded that when s-SPG interacts with relatively hydrophilic guest polymers, the resultant composites are always composed of two SPG polymers and one guest polymer.

2.2.4 Inclusion of Permethyldecasilane (PMDS)

Oligosilanes have been investigated as attractive functional materials, since they have unique σ-conjugated helical structures and show unique optoelectric properties [115–117]. Their fabrication using the one-dimensional cavity of SPG would be useful for various applications, such as (1) preparation of water-soluble oligosilane composites, (2) regulation of their helical conformation and (3) fabrication of their fibrous superstructures, etc. We have demonstrated that permethyldecasilane (PMDS, structure see: Fig. 3) is incorporated into the SPG cavity through our successful procedure to a one-dimensional composite, in which PMDS is indeed included inside the one-dimensional cavity of SPG [118]. Several lines of evidence including UV-VIS, CD and fluorescence spectroscopic data along with observations using a TEM and AFM have clearly revealed that water-soluble, helically ordered oligosilane-nanofibers are formed with s-SPG through the renaturation process.

Unlike the forgoing guest polymers, i.e., SWNT, PANI, PT, and PPE, all of which are soluble or dispersible either into water or into polar organic solvents, PMDS is soluble only in nonpolar organic solvents such as hexane. Accordingly, to prepare highly ordered PMDS/SPG composites with excellent reproducibility, establishment of a novel solubilization strategy is desired. A new biphasic procedure, on the basis of the renaturation process of s-SPG on the liquid/liquid interface, is thus exploited.

The triple strand of SPG is dissociated into the single strand at pH > 12, whereas it retrieves the original triple strand by pH neutralization [51]. Accordingly, in the present study, a NaOH solution containing s-SPG was neutralized by acetic acid, where the renaturing from s-SPG to t-SPG proceeds with decreasing pH values. Firstly, a hexane layer containing PMDS and an aqueous NaOH layer containing s-SPG were well homogenized by sonication. Aqueous acetic acid was then added to the resultant mixture to give two layers, where the renaturing from s-SPG to t-SPG would occur on the H_2O/hexane interface. The hexane layer thus obtained showed a broad UV-VIS absorption band with full-width-half-maximum (FWHM) of 40 nm around 280 nm, which is characteristic of the σ–σ^* transition of flexible, random-coiled PMDS. Detailed investigation of the concentration dependency of s-SPG indicated that the intensity at 280 nm in the hexane layer

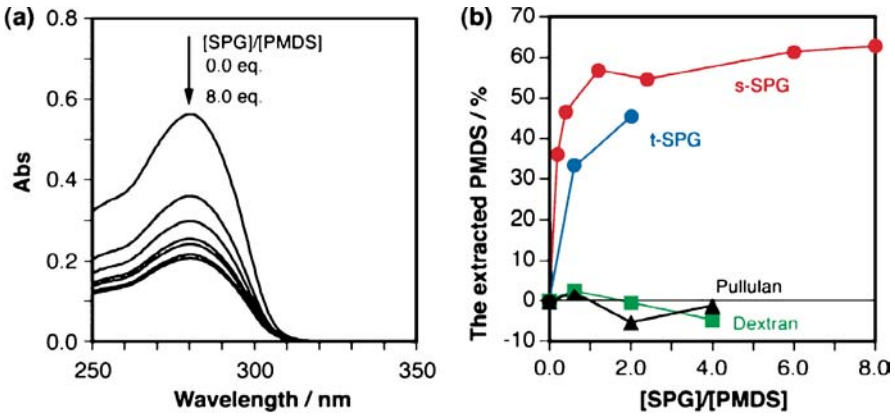

Fig. 22 **a** UV absorption spectra of the hexane layer after the treatment with aqueous layers containing different amounts of s-SPG and **b** Estimated percentages of PMDS extracted from the hexane layer into the aqueous one: pathlength 5 mm, 25 °C, [PMDS] = 0.431 mM (an original concentration in the hexane layers), [s-SPG] = 0.0–3.5 mM (0.0–8.0 eq., an original concentration in the aqueous layers) based on their repeating units (four glucoside units for SPG and one dimethylsilane unit for PMDS). Reprinted with permission from [118]

was diminished with increasing s-SPG concentration in the aqueous layer, where PMDS should be extracted into the aqueous layer with accompanying PMDS/SPG composite formation. The extraction efficiency reached ca. 60% at the highest s-SPG concentration (Fig. 22). The PMDS/SPG composite in a neutral aqueous solution showed an intense red-shifted fluorescence band with FWHM of 18 nm at 323 nm when excited at the σ–σ^* transition band (280 nm), compared to the corresponding fluorescence band at 310 nm of free PMDS in hexane.

Although the resultant aqueous layer showed the broad absorption band around 280 nm, no detectable CD signal was observed at this wavelength, suggesting that PMDS adopts a flexible, random-coiled conformation in the one-dimensional SPG cavity. From ^{1}H NMR analysis of the aqueous layer, i.e., in D_2O, PMDS and hexane are assumed to be co-included within the one-dimensional SPG cavity: in other words, PMDS is wetted by co-extracted hexane molecules (Fig. 23). Once the hexane layer was removed by lyophilization of the aqueous layer, followed by re-dissolution of the resultant PMDS/SPG composite into water, the resultant aqueous solution showed a sharp absorption band at 290 nm with a narrow FWHM of 12 nm as well as a positive CD signal at 283 nm and a negative one at 293 nm (Fig. 24). The small FWHM of this UV band suggests a very rigid, extended conformation of PMDS in the PMDS/SPG [119].

So far, detailed conformational studies on PMDS itself have been performed by using UV-VIS and CD spectroscopies. Accordingly, on the basis

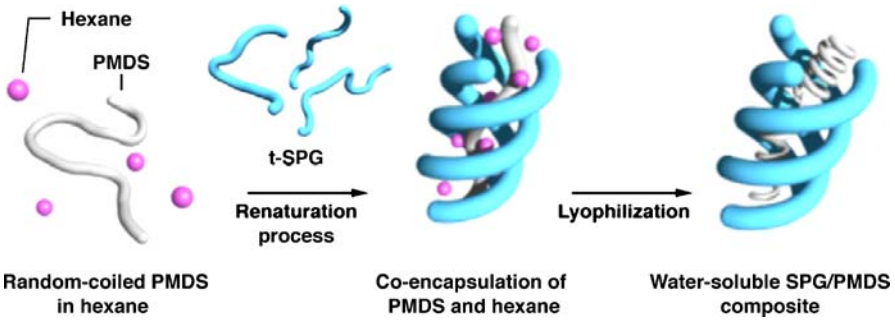

Fig. 23 Schematic illustration of the composite formation of s-SPG with PMDS. Reprinted with permission from [118]

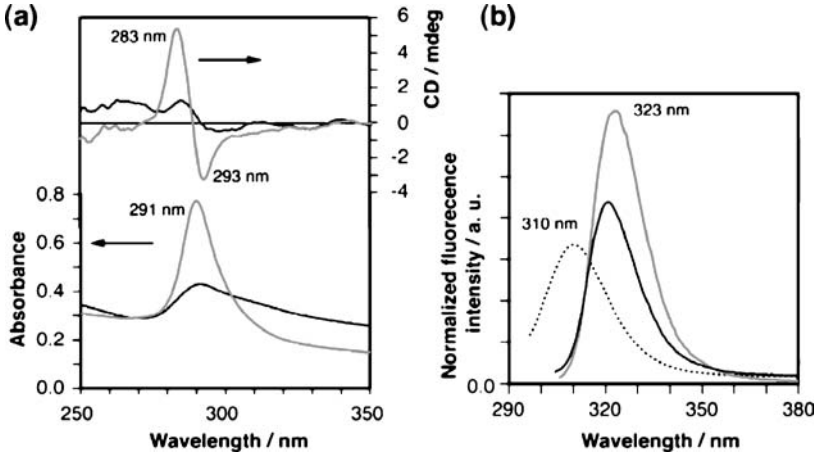

Fig. 24 **a** UV (*bottom*) and CD (*top*) and **b** Fluorescence spectra of the PMDS/SPG composite in water (λ_{ex} = 290 nm, *gray solid line*), the PMDS/t-SPG mixture in water (λ_{ex} = 290 nm, *black solid line*) and free PMDS in hexane (λ_{ex} = 280 nm, *black dotted line*): [s-SPG]/[PDMS] = 1.2 in molar ratio, cell length 0.5 cm and 25 °C. Reprinted with permission from [118]

of these reported results, it should be worth to compare the spectral feature of PMDS/SPG composite with PMDS itself, because the comparison would allow us to investigate how PMDS chain is wrapped by SPG. The origin of the bisignate CD spectral profile indicates two possibilities: (1) a mixture of two different helices with the opposite screw senses and different pitches and (2) exciton couplet due to chirally-twisted PMDS aggregates. Kunn's dissymmetry ratio being defined as $g_{abs} = \Delta\varepsilon/\varepsilon$ = CD (in mdeg)/32 980/Abs.), which is a dimensionless parameter to semi-quantitatively characterize helical structures of oligosilanes and other chromophoric chiral molecules, excludes the latter case, because the evaluated g_{abs} values at two extrema are

$+ 3.3 \times 10^{-4}$ at 283 nm and $- 1.7 \times 10^{-4}$ at 293 nm, respectively. The absolute magnitude in these small g_{abs} values is almost comparable with the g_{abs} value of (2.0–2.5) $\times 10^{-4}$ at 323 nm of rigid rod-like poly(silane) (PS) with a single-screw helix. PMDS incorporated in the helical cavity of s-SPG, therefore, exists as a mixture of diastereomeric helices with the opposite screw senses: the 283 nm CD signal is responsible for a P-7_3 helix and the 293 nm CD signal is for an M-15_7 helix. Additionally, UV-VIS and CD spectral features of PMDS/SPG composite are very similar to those for the PMDS/γCD composite [77].

2.3 Inclusion of Supramolecular Dye Assemblies

Having established the fundamental hosting abilities toward functional polymers, the one-dimensional hosting system was further extended to small molecular guests which possess potential abilities to self-assemble into one-dimensional supramolecular architectures. So far, creation of well-regulated supramolecular assemblies from a rationally designed dye molecule have attached the wide-spread interest in view of their potential applications for nonlinear optical and photorefractive devices [120–124]. A particularly challenging aspect is to create a wide variety of supramolecular assemblies from a single dye by using an appropriate template, on which dye molecules can be arranged in a well-regulated fashion to generate a wide variety of colors as well as functions, reflecting the higher-order structures of the template [10, 11, 19, 125–138].

A dipolar dye (azo-dye) having pyridine and carboxylic acid terminals has potential self-assembling capabilities through intermolecular interactions in addition to cooperative π–π stacking and dipolar–dipolar interactions [139, 140]. To achieve the different molecular arrangement of azo-dye molecule in the presence of SPG template, the different renaturing solvents, e.g., DMSO or NaOH solution were employed: in DMSO solution a self-assembling structure of azo-dye would be more dominated by the hydrogen-bonding interaction, whereas in NaOH solution π–π stacking and dipolar–dipolar interactions in addition to hydrophobic interactions would become major driving forces (Fig. 25).

As a first experiment, DMSO solution containing s-SPG was mixed with a DMSO solution of azo-dye followed by addition of water allowing renaturing to proceed. UV-VIS spectra of the azo-dye/SPG solution thus obtained was compared with azo-dye itself in the same solvent. The absorption maximum of azo-dye itself appears at 446 nm, whereas the peak of the composite is red-shifted to 468 nm [141]. This red-shift can be ascribed to the formation of J-type assemblies, promoted by the intermolecular hydrogen bonding in addition to π–π stacking interactions among azo-dye molecules. When a DMSO solution containing the azo-dye itself was diluted with water, the

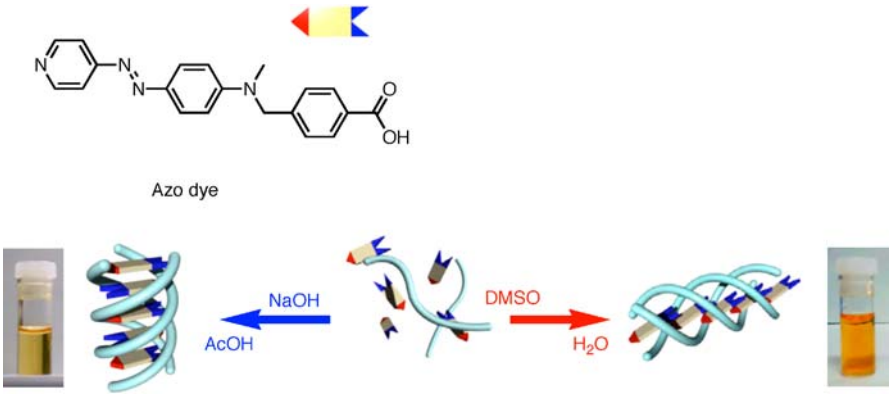

Fig. 25 Concept of the creation of supramolocular dye architectures showing "polymorphism". Structure of the designed dipolar dye with pyridine and carboxylic acid terminals. Reprinted with permission from [141]

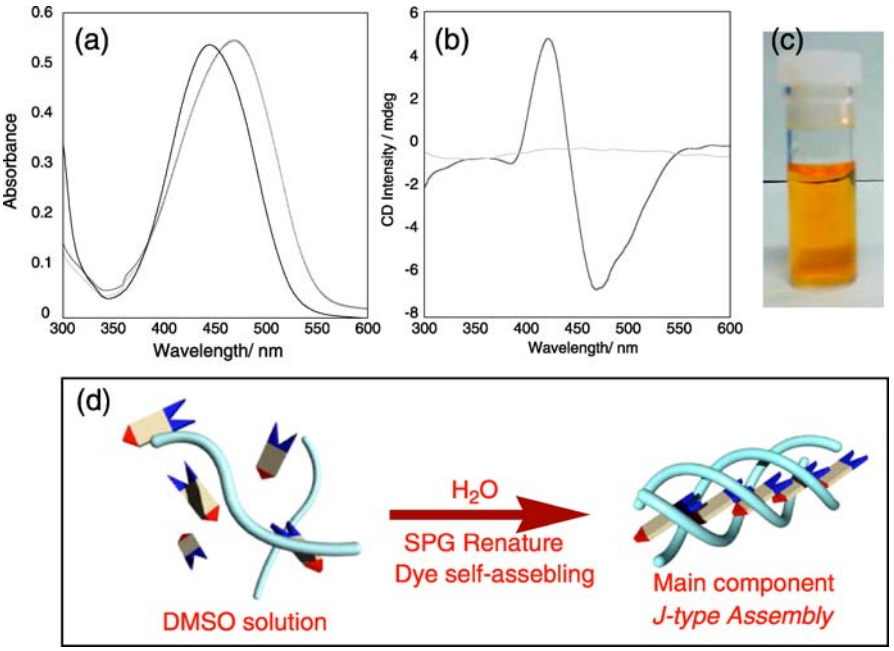

Fig. 26 **a** UV-VIS and **b** CD spectra of the samples containing azo dye/SPG composite (*black dotted lines*), monomeric azo dye in DMSO (*black line*) and azo dye aggregate in water/DMSO mixed solvent (*gray lines*), prepared from DMSO solution, 1.0 cm cell length, room temperature, **c** Photo image of the solution containing azo dye/SPG composite and **d** Schematic illustration of the J-type assembly formation during the renature of s-SPG: This type of assembly would be created as a major component in the solution. Reprinted with permission from [141]

mixture provided the precipitate after several minutes. When UV-VIS spectra of the temporarily "transparent" solution were taken immediately after addition of water, the absorption maximum appeared at 468 nm. These results support the view that a J-type assembly is entrapped into the SPG cavity. CD spectroscopy is helpful for monitoring the definitive interaction between SPG and azo-dye. Upon mixing with s-SPG an intense split-type ICD appeared in the π–π^* transition region of the azo-dye assembly. The self-assembling nanofiber structure of azo-dye is entrapped into the helical SPG cavity, adopting a twisted molecular arrangement (Fig. 26).

The triple strand of SPG is dissociated into the single strand at pH > 12, whereas it retrieves the original triple strand by pH neutralization. As an alternative strategy, we tried to construct a different type of azo-dye assemblies utilizing this neutralization process of the alkaline s-SPG solution, where π–π stacking and dipolar–dipolar interactions become the major driving forces instead of hydrogen-bonding interactions. To the NaOH solution containing

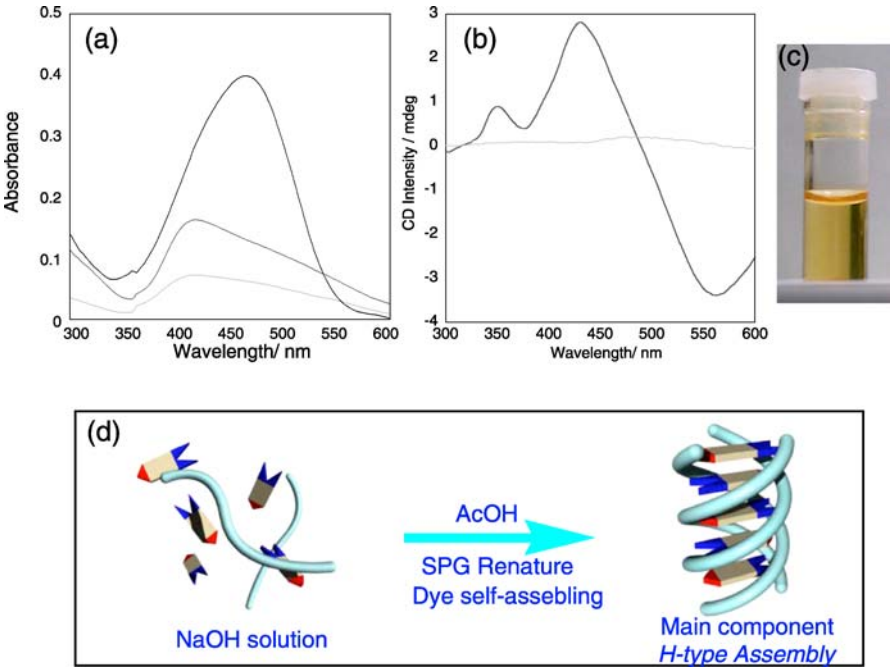

Fig. 27 **a** UV-VIS and **b** CD spectra of the samples containing azo dye/SPG composite (*black dotted lines*), monomeric azo dye in DMSO (*black line*) and azo dye aggregate in water/DMSO mixed solvent (*gray lines*), prepared from NaOH solution, 1.0 cm cell length, room temperature, **c** Photo image of the solution containing azo dye/SPG composite and **d** Schematic illustration of the H-type assembly formation during the renaturation of s-SPG: This type of assembly would be created as a major component in the solution. Reprinted with permission from [141]

s-SPG and azo-dye, aqueous acetic acid was gradually added to give a clear yellow solution, adjusting the final pH to 7. The absorption maximum of the solution is blue-shifted from 446 to 417 nm with accompanying slight peak broadening. This blue-shift is ascribed to the creation of the H-type assembly. Furthermore, ICD is also detected at the π–π^* transition region of the azo-dye assembly, indicating that the one-dimensional H-type assembly is entrapped in the helical SPG cavity, where π–π stacking and dipolar–dipolar interactions in addition to hydrophobic interactions would become the major driving forces (Fig. 27). It should be noted that the entrapped supramolecular structures of azo-dye are not affected by the solvent properties, meaning that the observed color changes are not due to the difference in solvent properties surrounding the composites. These results clearly support the view that the different dye assemblies can be created from azo-dye through the different preparation procedures. One may regard this phenomenon to be a sort of "polymorphism" induced by the presence of SPG. The creation of similar dye assemblies has been achieved by using porphyrin derivative, where a J-type porphyrin assembly is also entrapped into the helical SPG cavity [142].

2.4 β-1,3-Glucan as a One-Dimensional Reaction Vessel

Our research efforts are particularly focused not only on polymeric guests but also on low molecular weight compounds. Especially, it is of great significance to establish β-1,3-glucan-templated polymerization of various monomers in the one-dimensional cavity to construct the corresponding polymers with fibrous morphologies, where SPG or CUR is expected to act not only as a one-dimensional host for monomers but also as a one-dimensional vessel for the stereoselective polymerization reaction (Fig. 28). Herein, we show several successful examples where SPG accommodates various reactive monomers, including 1,4-diphenylbutadiyne (DPB) derivatives, EDOT and alkoxysilane, within the one-dimensional cavity and produces unique water-soluble nanofibers through in situ polymerization reactions.

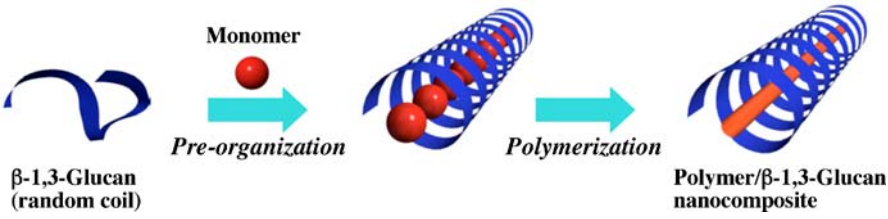

Fig. 28 Concept of in situ polymerization reaction utilizing β-1,3-glucan as a vessel

2.4.1
Photo-Polymerization of Diacetylene Derivatives

Poly(diacetylene)s are known as a family of the most interesting research targets among the π-conjugated polymers, because they are readily produced through photo-irradiation (UV or γ-ray) without any initiators [143–145]. Instead, for the photo-mediated polymerization of diacetylene derivatives, closely packed pre-organization of the corresponding monomers is indispensable [146–148]. Therefore, this topochemical polymerization process of diacetylene derivatives was mainly studied only in crystals, micelles and Langmuir–Blodgett films, where corresponding monomers are aligned in a parallel but slightly slided packing mode. In the present study, 1,4-diphenylbutadiyne (DPB) derivative was used as a monomer and pre-organization of DPB can be easily achieved by incorporation into the one-dimensional SPG cavity [149, 150].

The general procedures are as follows: a DMSO solution containing s-SPG was mixed with DPB DMSO solution and the resultant mixture was diluted with water to regenerate a t-SPG helical structure. Although DPB was scarcely soluble by itself in water, the resultant slightly turbid solution showed a clear CD spectrum, which is assignable to an absorption band of DPB. As reference experiments, when other polysaccharides and carbohydrate-appended detergents (amylose, pullulan, dextran, and dodecyl-β-D-glucopyranoside) were used instead of s-SPG, no or a negligibly weak CD signal was observed (Fig. 29). Together with the fact that SPG or DPB itself gave no CD signal at this wavelength region, the observed negative CD exciton-coupling is indicative of twisted-conformations or -packings of DPB arising from the strong helix-forming capability of SPG. These results support the view that DPBs are pre-organized only in the presence of s-SPG to form a one-dimensional supramolecular assembly, which is favorable to subsequent polymerization reaction under UV-irradiation.

UV-irradiation using a high-pressure Hg-lamp induced a gradual color change of the solution containing the DPB/SPG complex from colorless to pale blue. The UV-VIS spectrum of the resultant solution shows an absorption band at around 720 nm which is characteristic of poly(diacetylene)s with extremely long π-conjugated length and/or tight inter-stranded packing [151, 152]. UV-mediated polymerization of DPB was also confirmed by Raman spectra, in which the DPB/SPG complex shows a clear peak at 2000 cm^{-1} assignable to poly(diacetylene)s (–CH=CH– stretching vibration) after 16 h UV-irradiation. On the contrary, no such Raman peak appeared without SPG. Together with the fact that UV-mediated polymerization of diacetylenes proceeds in a topochemical manner, these data suggest that SPG accommodates DPB to align them in a packing suitable for such topochemical polymerization. It should be noted that *p*-amido-functionalities of DPB are essential for the UV-mediated polymerization. We assume that the *p*-amido-

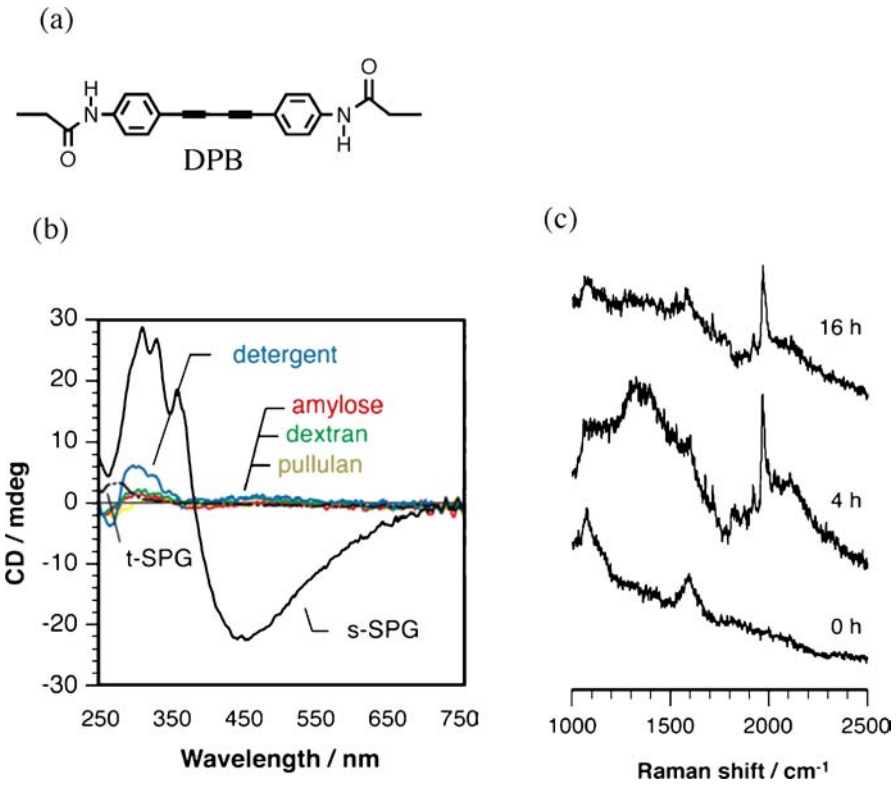

Fig. 29 **a** Structure of 1,4-diphenylbutadiyne (DPB) derivatives, **b** CD spectra of DPB in the presence of s-SPG, amylose, dextran, pullulan, t-SPG and the detergent: cell length 1.0 cm, 20 °C, [H_2O] = 70% v/v, [DPB] = 25 μg/ml, [polysaccharide] or [detergent] = 25 μg/ml, **c** Raman spectra of DPB in the presence of s-SPG after 0, 4 and 16 h

functionalities should form hydrogen-bonds with SPG and/or neighboring monomers to orientate the monomers in suitable packing arrangements for the polymerization. The results presented here will open a way to construct poly(diacetylene)-nanofibers with uniform diameters from various DPB-derivatives.

2.4.2 Sol–Gel Polycondensation Reaction of Alkoxysilane

Creation of supramolecular organic/inorganic hybrid materials has been of great concern in recent years [153–155]. In particular, inorganic nanofibers which have a well-regulated shape and high water-solubility, reflecting those of organic templates, are desired for potential applications to biosensors, switches, memories, and circuits [156–159]. So far, silica nanofibers have been created using the templating method where anionic silica particles are

deposited on a cationic fibrous template. However, the difficulties in surface modification, by which one may dissolve the organic/inorganic composite into the solvent, still remain unsolved because the solvophobic inorganic layer always exists outside the solvophilic organic template. It thus occurred to us that when hydrophobic metal alkoxides are entrapped in the one-dimensional SPG cavity, sol–gel polycondensation takes place inside the cavity to afford a silica nanofiber which shows the water-solubility as well as the biocompatibility arising from surface-covering SPG, making biological applications. Here, we carried out the sol–gel polycondensation reaction in the presence of s-SPG using TMPS (trimethoxypropylsilane) as a monomer [160].

TMPS was dissolved in DMSO and mixed in solution with s-SPG or s-CUR during the renaturing process. After leaving the mixed solution for 20 days at room temperature, the resultant water/DMSO mixed solvent was subjected to dialysis. The IR spectrum showed the appearance of a strong new vibration band assignable to the Si–O–Si bond at around the 1000–1200 cm^{-1} region. Interestingly, the obtained silica did not form any precipitate even after dialysis against water, indicating that the created silica is successfully wrapped by hydrophilic SPG or CUR.

The aqueous silica suspension obtained from the TMPS/SPG system was cast on a grid with carbon mesh and the morphologies of the obtained silica were observed by TEM. As expected, the fine silica nanofiber structure with a uniform 15 nm diameter is observed (Fig. 30), whereas no such fibrous structure is found from the sample prepared in the absence of SPG. From these TEM images, one can propose that sol–gel polycondensation of TMPS predominantly proceeds in the one-dimensional SPG cavity to afford silica nanofibers soluble in water. Furthermore, the diameter of the obtained silica nanofiber increased (ca. 25 nm) with the increase in the feed TMPS concentration up to TMPS/SPG repeating unit = 3.0 eq. However, when more than 3.0 eq. TMPS against s-SPG repeating unit was used, the silica nanofiber structure was no longer created and instead an amorphous silica mass was formed. The results support the view that under such a condition where TMPS exists in great excess, s-SPG cannot cover the original one-dimensional assembly structure of TMPS during the renaturating process, so that it can no longer act as the host effectively. The view is also supported by the fact that sol–gel polycondensation in the presence of t-SPG instead of s-SPG did not give any fibrous structure; that is, the renaturating process from s-SPG to t-SPG is indispensable for inclusion of TMPS followed by the creation of the silica nanofiber structure.

It is well-known that a catalytic amount of benzylamine or HCl allows the sol–gel polycondensation to proceed. In the present system, however, we could not find any fibrous structure from such reaction conditions. The result indicates that the very slow condensation reaction is favorable for one-dimensional growth of silica nanofibers. In fact, it took more than two weeks to create the complete nanofiber structure. Thus, to elucidate the reaction

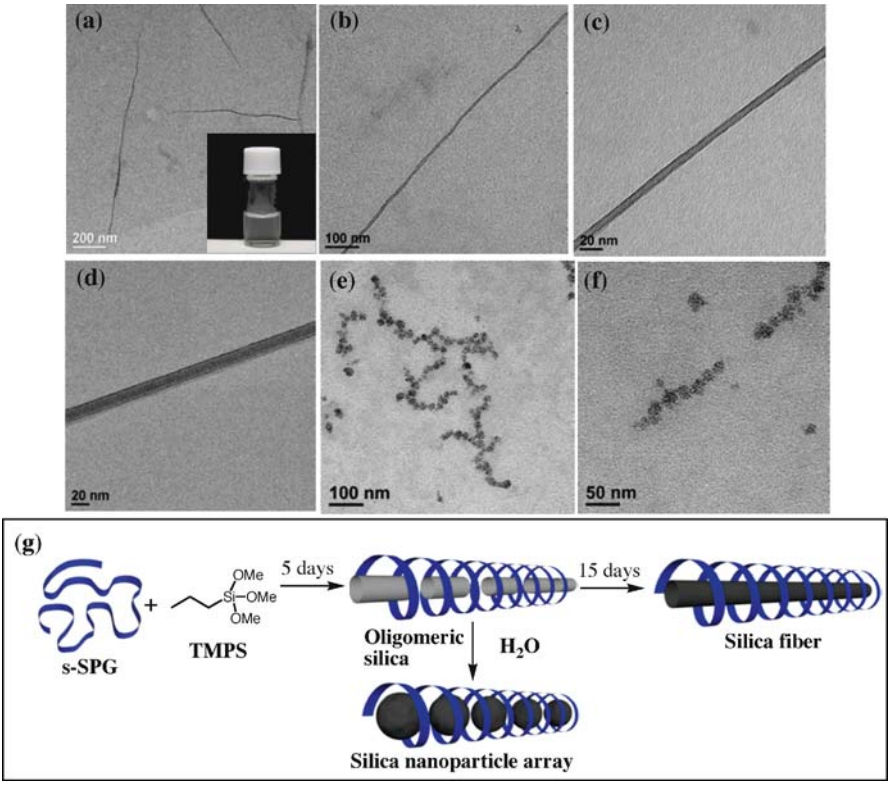

Fig. 30 **a** TEM image of silica nanofibers (*inset*: photo image of aqueous solution of silica nanofibers) (TMPS/SPG repeating unit = 1.0 eq.), **b**, **c** Its magnified images, **d** TEM image of silica nanofiber (TMPS/SPG repeating unit = 3.0 eq.), **e** TEM image of silica nanoparticle one-dimensional arrays, **f** Its magnified image and **g** Schematic illustration of our concept to utilize SPG as a vessel for sol–gel polycondensation reaction

mechanism of the polycondensation reaction, we stopped the sol–gel reaction only after 5 days and observed the morphologies of the obtained silica by TEM. Very interestingly, the morphology of the obtained silica is not a fiber but a one-dimensional array of silica nanoparticles with 10–15 nm. Here, one can propose the possible growth mechanism as the following; that is, SPG acts as a one-dimensional host for TMPS or its oligomers and the polycondensation occurs inside the cavity to give rod-like oligomeric silica after 5 days. This rod-like oligomeric silica is easily destroyed and finally converted into particles during the dialysis process due to the hydrophobic interaction among propyl groups. These results strongly support the view that SPG and CUR have a potential ability to act not only as a one-dimensional host for TMPS but also as a vessel for sol–gel polycondensation reactions. We believe that the present system would be readily applicable to the creation of novel organic/inorganic hybrid nanomaterials and their functionalized derivatives.

2.4.3
Chemical Polymerization of 3,4-Ethylenedioxythiophene (EDOT)

Poly(3,4-ethylenedioxythiophene) (PEDOT) has been widely investigated during the past decade owing to its low band gap, high conductivity, good environmental stability, and excellent transparency in its oxidized state [161–164]. More recently, the preparation and characterization of PEDOT nanostructures have become a topic of increasing interest due to their potential applications to electrical, optical, and sensor devices [165–169]. On the basis of the established one-dimensional hosting abilities of β-1,3-glucans, herein, we carried out a polymerization reaction of EDOT in the presence of s-SPG initiated by the oxidant ammonium persulfate (APS), expecting that PEDOT nanofibers are created in the SPG cavity [170]. After the polymerization reaction, homogeneous and stable aqueous dispersions with a dark blue color were obtained. Subsequently, the aggregated structure of the PEDOT/SPG composites was examined by TEM (Fig. 31). Unexpectedly, it is clearly seen from the TEM images that the resultant composite does not construct PEDOT nanofibers but PEDOT nanoparticles with uniform size and regular shape. Interestingly, when the concentration of used SPG increased, the diameter of the nanoparticles decreased from 160 nm ([s-SPG] = 0.5 mg/ml) to 70 nm ([s-SPG] = 3.0 mg/ml), indicating that SPG acts as a template for the polymerization reaction. Further reliable evidence that s-SPG really acts as the template for the particle formation was obtained from the energy dispersive X-ray spectroscopy (EDS); that is, the O/S elements ratio in the nanoparticle clearly shows that PEDOT and SPG coexist in the created nanoparticles.

To elucidate the growth mechanism of PEDOT/SPG nanostructures, CD spectra of the resultant solution were recorded. The CD spectra revealed that PEDOT/SPG nanoparticles show no CD signal, suggesting that no effective interaction occurred between SPG and PEDOT. This fact leads us to the conclusion that at the initial stage, the polymerization of EDOT proceeds mainly in the bulk phase due to the good solubility of EDOT in water/DMSO mixed solvent. On the other hand, PEDOT is hydrophobic and insoluble in water/DMSO mixed solvent. Therefore, once PEDOT is formed, the polymer chains tend to aggregate through the strong intra- or intermolecular π-stacking. Consequently, the hydrophobic EDOT oligomer or polymeric PEDOT with the entangled polymer backbone may interact with s-SPG to form the PEDOT/SPG complex, where SPG cannot act as an effective one-dimensional template for such globular-shaped polymeric guests. It is worth mentioning that the PEDOT/SPG composite would act as a sort of amphiphilic block copolymer, which can self-aggregate into nanoparticles under the experimental conditions. This unexpected result would provide novel methodologies to create water-soluble PEDOT nanoarchitectures.

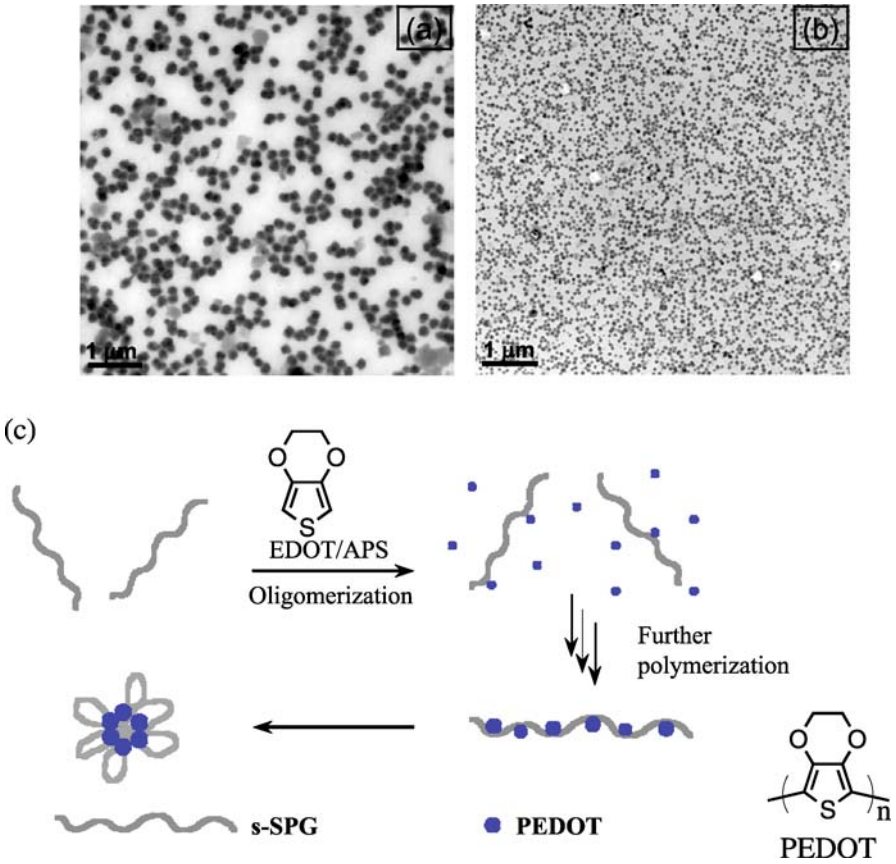

Fig. 31 TEM images of PEDOT/SPG nanoparticles prepared by APS oxidant in the presence of s-SPG ([EDOT] = 9.4 mM, [APS] = 94 mM): **a** [SPG] = 0.5 mg/ml, **b** [SPG] = 3.0 mg/ml and **c** Schematic illustration of the possible growth mechanism of water-soluble PEDOT/SPG nanocomposites

2.5 One-Dimensional Arrangement of Au-Nanoparticles

Nanoscale assemblies of inorganic nanoparticles, consisting of a limited number of metal or semi-conductive nanoparticles, have received considerable attention in recent years due to their application as nano- and biomaterials, e.g., sensors, memory, imaging agents, etc. [171–174]. Such inorganic nanoparticles, however, lack the potential abilities to arrange along specific directions as atoms or organic hybrids. Control of the self-assembling behavior of nanoparticles is, therefore, a still challenging research subject and exploitation of the versatile strategy is strongly desired [175].

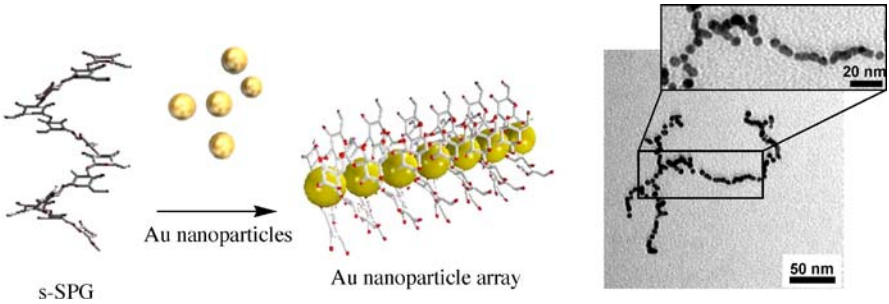

Fig. 32 TEM images of Au nanoparticle arrays

The unique renaturing process during the guest encapsulations provides one great advantage of SPG, that is, a flexible, induced-fit-type size/shape-selectivity for the guests, independent of the surface nature of the guests. This advantage of SPG is clearly demonstrated by using Au nanoparticles as a guest [176]. For example, stable Au/SPG composites were obtained from commercially available Au nanoparticles (5–50 nm). The resultant Au/SPG composites are well-soluble in water but show a significantly broadened plasmon absorption, indicating SPG-induced assemblies of Au nanoparticles in aqueous media. TEM observations of the resultant Au/SPG composites showed unique one-dimensional Au nanoarrays with their length consistent with that of s-SPG itself. These data clearly indicate that the one-dimensional nanoarrays of Au nanoparticles arise from their encapsulation within the one-dimensional cavity of SPG (Fig. 32).

SPG will act not only as a one-dimensional template for preorganization of Au nanoparticles but also for facilitation of fusion of Au nanoparticles [177].

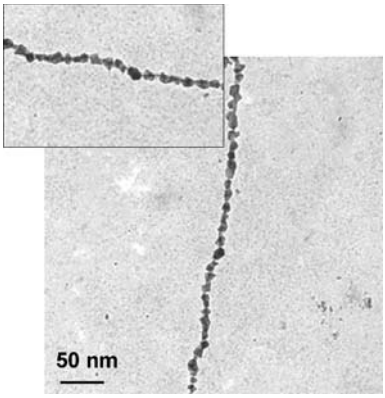

Fig. 33 TEM images showing formation of continuous nanowires: Au nanowires created using chemical reduction of $HAuCl_4$ after pulsed-laser irradiation in aqueous solution at 25 °C; 5 min, 5 mJ/pulse, 532 nm

We have found that a morphological change of one-dimensionally aligned SPG-Au composite is induced by 532 nm laser irradiation, which leads to the fusion of Au nanoparticles to prepare discontinuous Au nanowires. Furthermore, using both the near-IR irradiation and a reducing agent lead to continuous Au nanowires. This capability opens up new possibilities not only for novel sensor systems but also for applicant electronics, for example, patterning the metallization in solution for nanocircuits, which was previously very difficult (Fig. 33).

3
Chemically Modified β-1,3-Glucans

3.1
Synthetic Strategies Toward the Selective Modification

Many polysaccharide researches have focused on exploiting the functional material thorough chemical modification of polysaccharides. The problems in chemical modification of natural polysaccharide arise from the similar reactivity of the hydroxy (OH) groups, making selective functionalization difficult. Accordingly, to introduce functional groups into the desired OH groups, much effort has been paid to exploiting an effective synthetic route, facilitating access to various polysaccharide-based nanomaterials.

Chemical modification of β-1,3-glucans has been independently developed by several research groups including us [178–194]. Here, to prepare the functionalized β-1,3-glucan one-dimensional hosts, the selective modification targeting to side-glucoses for SPG and 6-OH groups for CUR need to be exploited, because 2- or 4-OH groups connected to the main-chain glucose units are indispensable for the construction of the inherent helical structure [1]. On the basis of this fact, we successfully established a versatile synthetic route to introduce various functional groups selectively into the side-glucoses of SPG and 6-OH groups of CUR, without affecting the inherent helix-forming properties of β-1,3-glucans (Schemes 1 and 2).

CUR has one primary OH group in its repeating unit, appending at C-6, i.e., the 6-OH group, which would be an active nucleophile under appropriate reaction conditions, making the selective modification of 6-OH groups possible. Moreover, the quantitative reaction can be achieved through the azideation reaction of 6-OH, followed by "click chemistry", which involves a Cu(I)-catalyzed chemoselective coupling between organic azides and terminal alkynes [192, 193]. This newly exploited strategy allows us to directly introduce various functional groups into 6-OH groups of CUR, leading to the creation of functional materials based on CUR (Scheme 2). Actually, we have successfully developed that 6-OH groups of CUR are convertible to various functional groups, e.g., ferrocene, pyrene, phorphyrin, trimethylammonium,

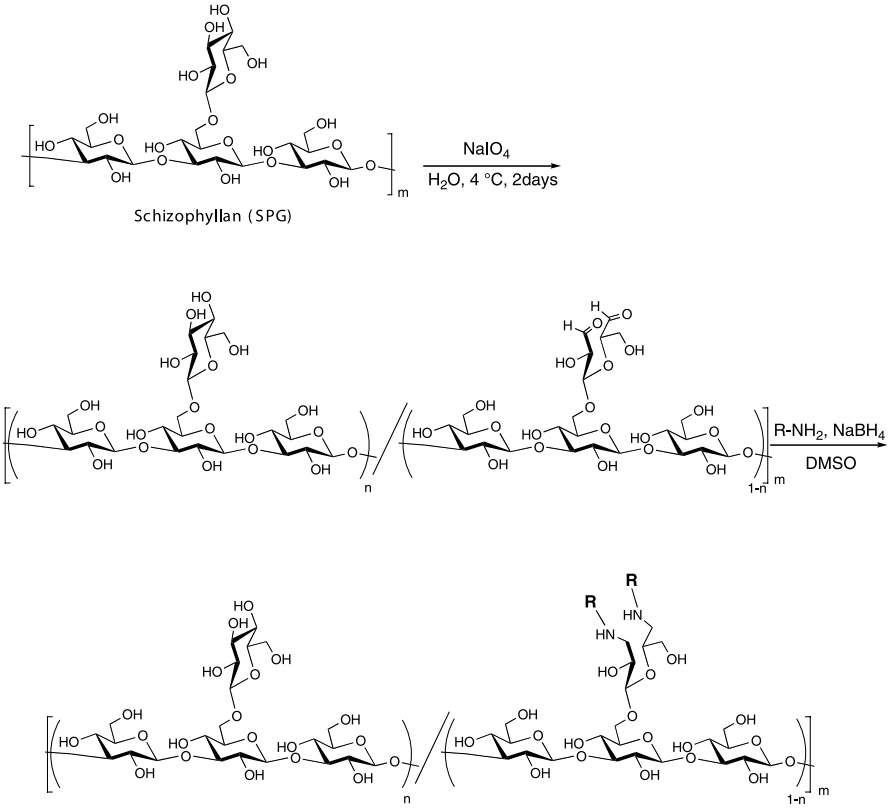

Scheme 1 Synthetic strategy for the selective modification of SPG side glucoses

sulfonate, etc., and found that these functional groups in the side chains govern the chemical properties of the modified CUR [185, 186, 192–194]. The advantageous point of this method is that a series of reactions proceed quantitatively and selectively. Additionally, by adjusting the feed acetylene composites, different functional groups are easily introduced into the same CUR chain in a step-wise manner.

SPG has two primary OH groups on the main chain and side glucose groups, so that the selective modification targeting to the primary OH groups seems to be difficult. On the other hand, the side glucose groups of SPG have 1,2-diols at 2-, 3- and 4-OH positions, whereas main chain glucoses have no such 1,2-diol due to the glicoside linkage formation between 1- and 3-OH positions. Therefore, one may expect that the oxidative cleavage of these 1,2-diols by $NaIO_4^-$ would proceed selectively only at the side glucose units. Combining this oxidative cleavage of the 1,2-diols with the reductive amination reaction, these classical synthetic strategies can be a powerful tool for the selective modification of the native SPG chain (Scheme 1). So far, we

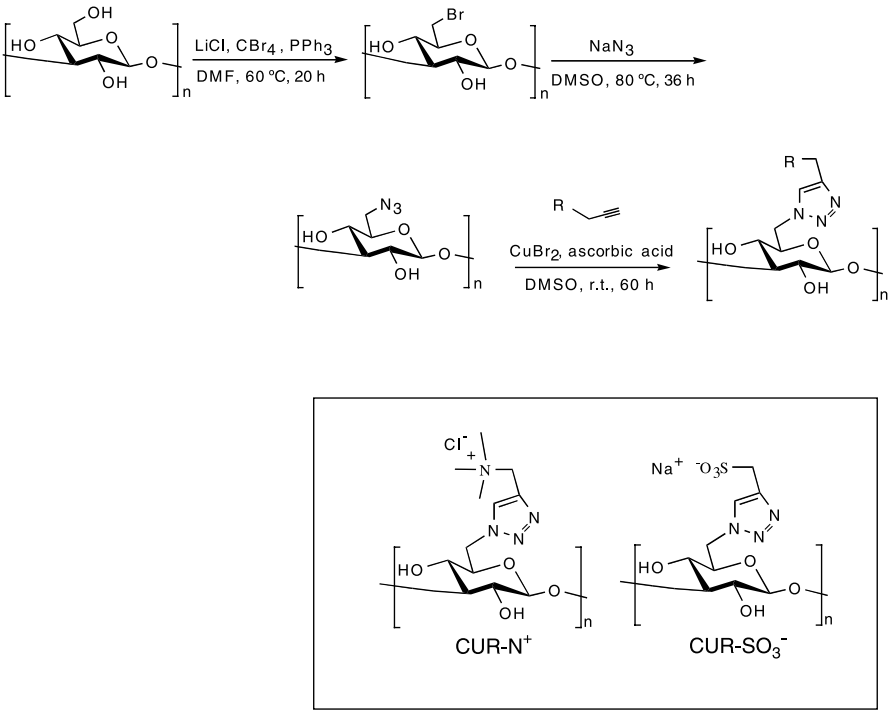

Scheme 2 Synthetic strategy for the selective modification of CUR 6-OH groups

have demonstrated that a series of chemically modified SPGs bearing various molecular recognition moieties, e.g., ionic groups, saccharide, amino acid, co-enzyme, etc., can be successfully obtained according to this synthetic strategy [184, 187–191]. Here, it should be important to address the discrepancy between these chemically modified CURs and SPGs: 6-OH groups of CUR can be converted to functional groups "quantitatively", whereas the side glucose groups of SPG can be "partially" functionalized because excessive oxidation of the side glucoses causes the insoluble aggregate probably due to the interpolymer cross-linking between 6-OH and aldehyde groups thus formed. The modification percentage of the side glucose groups is, at most, 30%.

3.2 Partially Modified SPG: One-Dimensional Host Toward the Supramolecular Functionalization of Guest Polymers

When polymeric guests or molecules are entrapped into the SPG cavity, the side group glucose should exist on the surface of the composites. If this is the case, a functional group introduced into the side group glucose would be useful as a recognition target. To test this idea, according to the reported

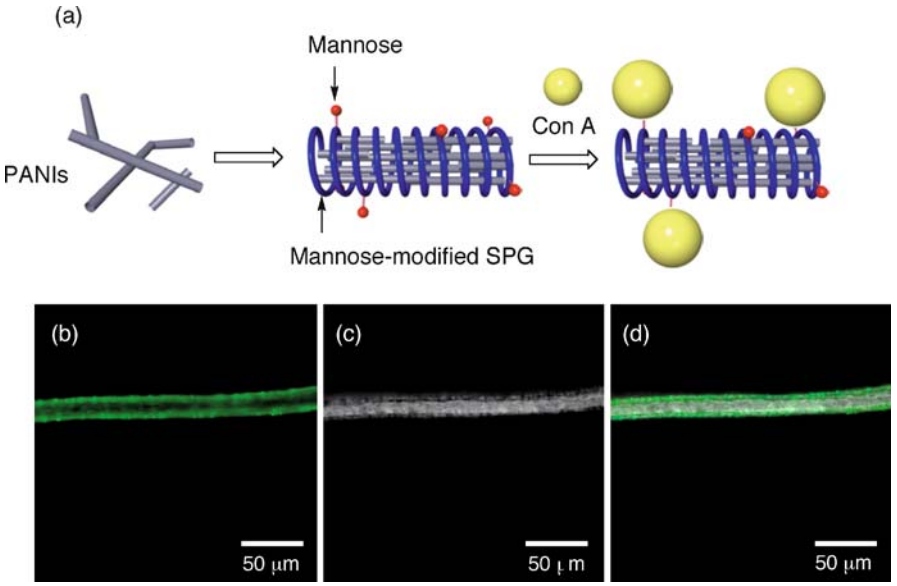

Fig. 34 **a** Concept of the supramolocular functionalization of the entrapped guest polymers. CLSM images of PANIs/mannose-modified SPG composite + FITC-ConA, **b** Fluorescence image, **c** Optical microscope image, **d** Overlap of (**b**) and (**c**). Reprinted with permission from [97]

procedure, mannose-modified SPG was synthesized and used as a wrapping reagent for PANIs [97]. It is known that this mannose group exhibits selective binding to Concanavalin A (ConA). Actually, the specific interaction between the composite and ConA was estimated by a CLSM using a FITC-labeled ConA (Fig. 34). The CLSM observation clearly shows that PANIs and ConA coexist in the same domain, indicating that (1) mannose-modified SPG can also wrap PANIs and (2) the mannose groups introduced into the side groups would exist on the exterior surface of the composite.

The findings clearly show that chemically modified SPG maintains its inherent ability as a one-dimensional host. The wrapping of the chemically modified SPG provides a novel strategy to create functional polymer composites in a supramolecular manner. Considering a general difficulty in introducing functional groups into the functional polymer backbones, the present system can be a new potential path to develop functional polymeric materials.

3.3
Semi-Artificial Polysaccharide Host Based on CUR

Even though the selective modification at 6-OH of CUR does not affect its inherent helix-forming ability, the renaturation and denaturation properties as well as the solubility of the modified CURs are strongly affected by the na-

ture of the introduced groups, because they always exist on the helix surface. Among various functional groups introduced into 6-OH groups, so far, ionic groups, such as trimethyl ammonium and sulfonium groups are of significant interest: the electrostatic repulsion among the ionic groups on the CUR surface would provide strong influence on its conformation in water, because the ionic groups are located in the distance of approximately 6 Å if they adopt the triple-stranded helical form. Consequently, the electrostatic repulsion causes the destabilization of the triple helix, being transformed to a loosely tied triple-stranded or to a single-stranded conformation in water. This fact implies that the modified CURs have potential for acting as a one-dimensional host even without the denaturation/renaturation processes in water.

To confirm the conformational properties of CUR-N^+, we measured the optical rotatory dispersion (ORD) spectra at various conditions (Fig. 35A). In the form of a triple-stranded helix, the ORD spectra of β-1,3-glucan polysaccharides such as SPG and CUR have positive values at the wavelength region from 600 to 200 nm. However, CUR-N^+ in water shows a negative sign at this

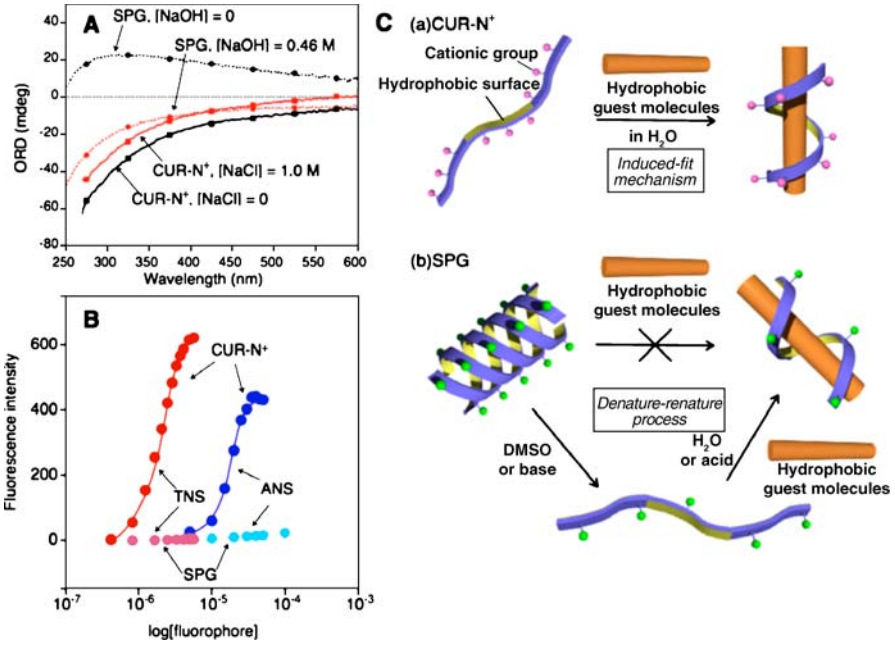

Fig. 35 **A** ORD curves of CUR-N^+ and SPG in aqueous solution (5 mg/ml) at various conditions at 25 °C, **B** Plots of fluorescence intensities at 480 nm for ANS (λ_{ex} = 370 nm) and at 450 nm for TNS (λ_{ex} = 370 nm) versus log fluorophore concentration in the presence of CUR-N^+ [10 μM (monomer unit)] or SPG [10 μM (monomer unit)] in aqueous solution at ambient temperature and (**C**) Schemes showing composite formation between β-1,3-glucans [(a) CUR-N^+ and (b) SPG] and a hydrophobic guest molecule. Reprinted with permission from [192]

wavelength region. The negative sign can be ascribed to the single-stranded form. In addition, we evaluated the effect of added NaCl on the ORD sign of CUR-N^+, expecting that it may reduce electrostatic repulsion. Interestingly, the intensity of ORD increased gradually with increasing NaCl concentration but did not reach the value of SPG in water. This difference implies that formation of the triple-stranded helical structure from CUR-N^+ is strongly suppressed by electrostatic repulsion among the cationic charges of the side chains.

These findings are successfully supported by the fluorescence probe experiments using 1-anilinonaphthalene-8-sulfonate (ANS) and 2-*p*-toluidylnaphthalene-6-sulfonate (TNS) (Fig. 35B); that is, the fluorescence intensity of ANS and TNS was remarkably increased in the presence of CUR-N^+ or CUR-SO_3^- accompanied with the blue shift of the fluorescence maxima. These results indicate that ionic CURs can accommodate ANS (or TNS) molecules into the hydrophobic domain *even in water*, where ionic CURs exert their hosting abilities in their single-stranded forms. Native SPG and CUR never exhibit such abilities in water due to their inherent nature to form the stable triple helix. SPG with cationic moieties in its side glucoses, whose modification ratios reaches 30%, also shows similar behavior in water because of its still stable triple helix. These facts lead to the conclusion that the quantitative modification of 6-OH groups with ionic groups provide a unique and unusual nature to native β-1,3-glucans [192]. The advantageous lines for CUR-N^+ and CUR-SO_3^- as a one-dimensional host are that these CURs can act as one-dimensional hosts in water without denaturation/renaturation processes: unlike native or partially modified β-1,3-glucans, hydrophobic polymers as well as molecules can be easily entrapped into the hydrophobic domain through a simple mixing procedure (Fig. 35C).

This unusual hosting system was further applied for the polymeric guests, i.e., polycytidylic acid [poly(C)], permethyldecasilane (PMDS) and single-walled carbon nanotubes (SWNTs), which can be incorporated into SPG and CUR only through the denaturation/renaturation processes [68, 69, 84, 86, 118]. Upon just mixing these hydrophobic guest polymers with CUR-N^+ (or CUR-SO_3^-) in water, clear aqueous solutions were obtained. The characterization by UV-VIS, CD spectroscopic measurements (Fig. 36), and AFM and TEM observations revealed that these polymeric guests are entrapped into the hydrophobic domain to give stoichiometric, nanosized fibrous structures. In the case of a poly(C) guest, the complexation would be driven by the cooperative action of (1) the hydrogen-bonding interaction between the OH group at the C2 position and hydrogen-bonding sites of the cytosine ring, (2) the electrostatic interaction between the ammonium cation and the phosphate anion, and (3) the background hydrophobic interaction. Likewise, the binding properties of CUR-N^+ toward PMDS and SWNT are attributed to the one-dimensional amphiphilic nature of CUR-N^+ in water. In the case of PMDS, approximately 5% of PMDS feed can

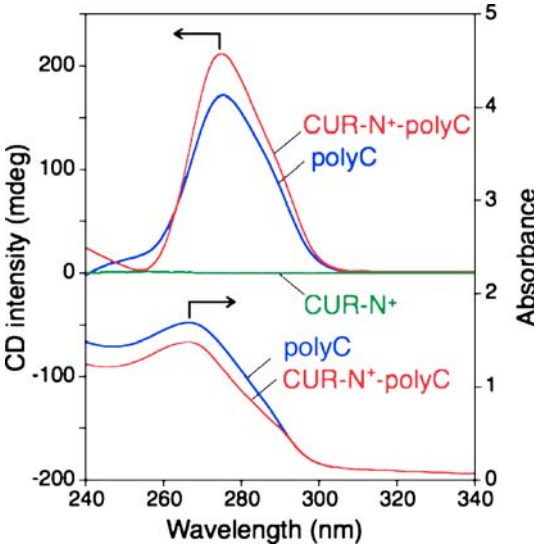

Fig. 36 UV-VIS and CD spectra of CUR-N^+ [1.3 mM (monomer unit)], poly(C) [0.24 mM (monomer unit)] and poly(C)/CUR-N^+ [1.3 mM (monomer unit), 0.24 mM (monomer unit)] in 1.0 mM tris-HCl buffer (pH 8.0) at 5 °C with a 1.0 cm cell (CUR-N^+ + poly(C) in absorption spectra corresponds to the sum of the individual spectra). Reprinted with permission from [192]

be solubilized into water by incorporation into the CUR-N^+ cavity. This value indicates that approximately 0.8 eq. of PMDS against CUR-N^+ in the monomer unit ($SiMe_2$ unit for PMDS and glucose unit for CUR-N^+, respectively) is included in PMDS/CUR-N^+ composites. Further conformational investigation of PMDS by CD spectroscopies reveal that the dissymmetry ratios (g) of PMDS/CUR-N^+ composites are smaller by a factor of ca. 4 than those of PMDS/SPG composites, indicating that the PMDS included in CUR-N^+ consists of a mixture of a few conformations (Fig. 37A). Together with the broad absorption band of PMDS/CUR-N^+ composites compared to that of PMDS/SPG composites, the strong electrostatic repulsion among cationic side-chains of CUR-N^+ probably prevents PDMS/CUR-N^+ composites from formation of a rigid supramolecular helical structure as seen in the PMDS/SPG system.

Powder of ag-SWNTs can be easily dispersed into water in the presence of CUR-N^+ or CUR-SO_3^- with the aid of sonication, the solution color becoming dark as the sonication time progressed. The resultant aqueous solution is stable for more than one-month without forming any precipitate probably due to the electrostatic repulsion among the composites. The NIR-VIS spectral feature of the solution was similar to that of the SWNT/SPG composite solution, suggesting that CUR-N^+ would wrap an individual SWNT fiber in the helical cavity. The fact is also supported by TEM and AFM observations (Fig. 37B).

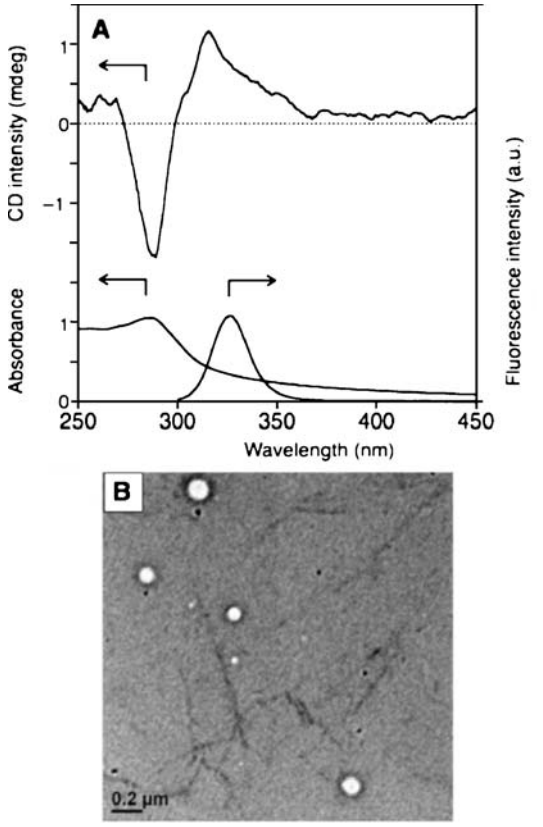

Fig. 37 **A** UV-VIS, fluorescence (λ_{ex} = 290 nm) and CD spectra of PMDS/CUR-N^+ composite ([CUR-N^+] = 3.0×10^{-4} M (monomer unit)), [PMDS] = 2.5×10^{-4} M (monomer unit); in an aqueous solution at ambient temperature and **B** The TEM image of PMDS/CUR-N^+ composite after treatment with phosphotungstic acid. Reprinted with permission from [192]

As described in the previous section, mannose-modified SPG can bestow the lectin affinity to PANI fibers by just wrapping them. The wrapping of the guest polymer by the chemically modified SPG can be regarded as a novel functionalization path through a supramolecular manner, where introduced functional groups always exist on the composite surface. Along the same lines, it is worth mentioning that an important aspect for the use of the chemically modified CUR is to functionalize the incorporated guest polymers by just wrapping them. In particular, the quantitative conversion of 6-OH groups to self-assembling groups allows the resultant composite to self-organize through the surface–surface interactions among the composites, where one-dimensional composites act as building blocks for creating the further hierarchical architecture.

4 Hierarchical Assemblies: The One-Dimensional Composite as a Building Block Toward Further Organization

Creation of highly ordered assemblies using functional polymers as building blocks, which would lead to novel chemical and physical properties depending on their assembling modes, is of great interest due to their potential applications as fundamental nanomaterials. The self-assembling system of small molecules have been well-established [195], whereas only a few attempts have been reported for the creation of such hierarchical architectures from polymers [196–198]. The difficulty in the polymeric system arises from how one can introduce self-assembling capabilities into a polymer backbone without losing its inherent functionality and from how one can assemble polymers through specific interpolymer interactions without the influence of the nonspecific bundling nature. Furthermore, to tune physicochemical properties of polymer assemblies at nanoscale, individual polymers must be manipulated during their self-assembling processes. The unique hosting ability of β-1,3-glucans has several advantages for overcoming these difficulties in polymer manipulation: that is, (1) when chemically modified β-1,3-glucans are used as one-dimensional hosts, the exterior surface of the resultant nanocomposites can be utilized as an interaction site for the construction of supramolecular architectures and (2) the strong interpolymer interactions among guest polymers are perfectly suppressed by the wrapping effect of β-1,3-glucans, which insulates one piece of guest polymer to maintain its original functionality. As a preliminary example, two kinds of complementary semi-artificial CURs, i.e., CUR-N^+ and CUR-SO_3^- were utilizing as a functional sheath for SWNTs, expecting that the mixture of these two composites in an appropriate ratio results in the creation of hierarchical SWNT architecture due to the electrostatic interaction [199]. It would be important to mention here that CUR-N^+ and CUR-SO_3^- have similar wrapping capability for SWNTs, suggesting that SWNT/CUR-N^+ composite and SWNT/CUR-SO_3^- composite may be used as "complementary" one-dimensional building blocks to create higher-order hierarchical self-assembled architectures (Fig. 38).

SWNT/CUR-N^+ and SWNT/CUR-SO_3^- composite solutions containing the same concentration of SWNT were prepared according to the same procedure described in the previous section. The zeta-potential value of an aqueous solution containing SWNT/CUR-N^+ composite was estimated to be + 48.9 mV, whereas an aqueous solution containing SWNT/CUR-SO_3^- composite showed – 49.5 mV. Once these two solutions were mixed in the same volume under very diluted conditions, the zeta-potential value of the resultant mixture showed – 0.53 mV without accompanying precipitate formation, indicating that the potential charges on these composites are almost neutralized to give a self-assembling composite through the electrostatic interaction.

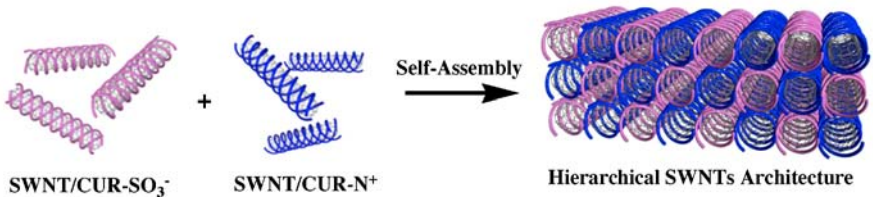

Fig. 38 Proposed concept for creating hierarchical SWNT architecture from one-dimensional building blocks through electrostatic interaction. It should be noted that all processes including wrapping of SWNTs by CUR and self-assembling of the resultant composites proceed in a supramolecular manner. Reprinted with permission from [199]

AFM images revealed that the resultant solution contains a well-developed sheet-like structure with micrometer-scale length, which is entirely different from the very-fine fibrous structures observed for individual SWNT/CUR-N^+ and SWNT/CUR-SO_3^- composites (Fig. 39). These sheet-like structures show the characteristic Raman peaks at 262 and 1592 cm^{-1} being ascribed to SWNTs.

TEM is a powerful tool to study how SWNTs are arranged in the obtained sheet-like structure. In the TEM images shown in Fig. 40, it can be recognized that the sheet-like structure is composed of highly ordered fibrous assemblies. Furthermore, the electron diffraction pattern (inset in Fig. 40B) reveals that the fibrous assembly has some crystalline nature, suggesting that cationic and anionic composites are tightly packed through the electrostatic interaction. The periodicity of the dark layer is estimated to be ca. 2 nm, which is almost consistent with the diameter of the individual composite obtained by the AFM height profile. These results reasonably lead to the conclusion that a novel strategy toward the creation of "hierarchical" functional polymer architectures can be established by utilizing the complementary semi-artificial β-1,3-glucans as "building blocks".

The mixture of the oppositely charged small molecules tends to result in nonspecific irregular assemblies through electrostatic interactions, but when either a cationic or anionic polymer exists excessively, specific regular structures with well-controlled size and assembling number can be created. This concept may be applicable to the present polymer assembling system. When an aqueous SWNT/CUR-N^+ composite solution was mixed with an excess amount of an aqueous SWNT/CUR-SO_3^- composite solution, adjusting the [SWNT/CUR-N^+]/[SWNT/CUR-SO_3^-] ratio to 1/5, bundled SWNTs architectures composed of highly ordered fibrous assemblies were obtained. The diameter of the bundle structure became larger, with increasing [SWNT/CUR-N^+]/[SWNT/CUR-SO_3^-] ratio from 1/5 to 1/3. These results indicate that the self-assembling hierarchical architecture is predictable and controllable by tuning the ratio of SWNT/CUR-N^+ composite and SWNT/CUR-SO_3^- composite (Fig. 41).

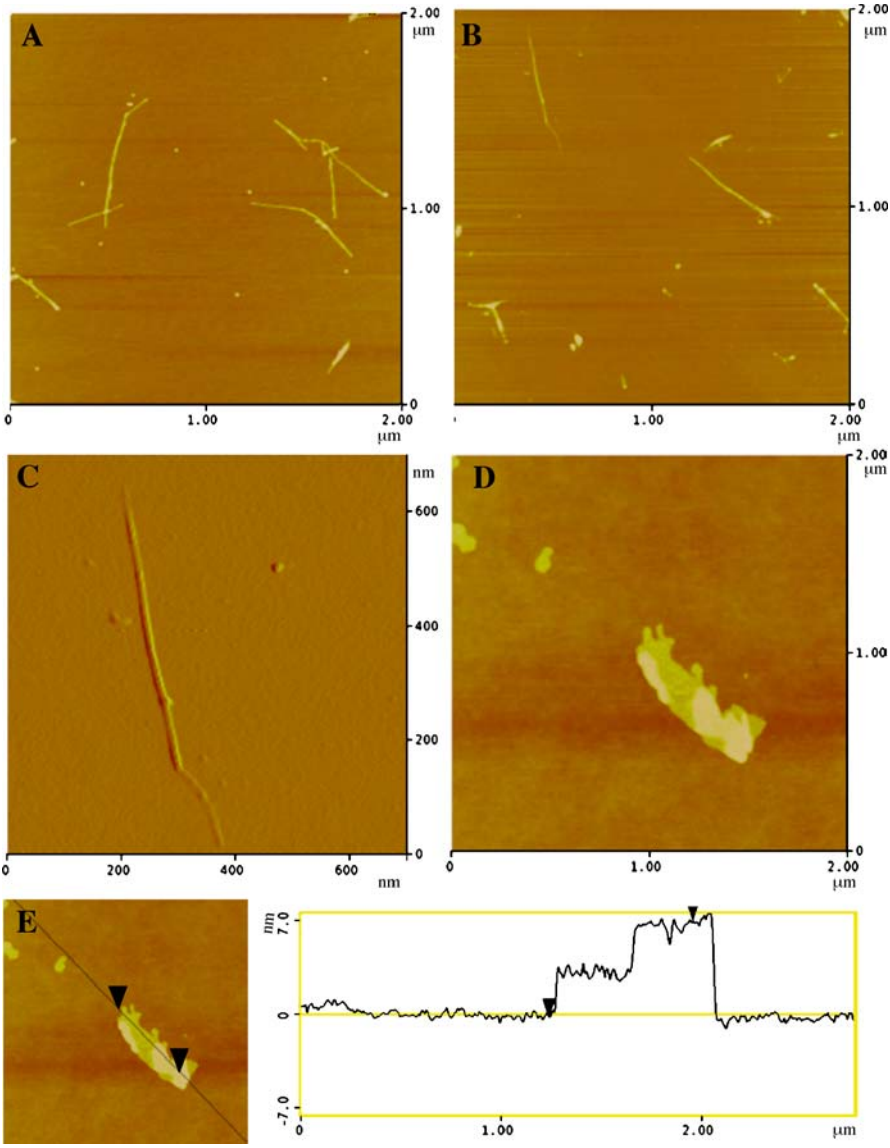

Fig. 39 AFM images of **A** SWNT/CUR-N^+ composite and **B** SWNT/CUR-SO_3^- composite, respectively. **C** Magnified AFM image of (**B**). **D** AFM image of the sheet-like structure after mixing SWNT/CUR-N^+ composite and SWNT/CUR-SO_3^- composite. **E** Height profile of the sheet-like structure: the AFM tip was scanned along the *black line*. In this AFM image, the thickness of each thin layer is estimated to be ca. 3.5 nm. Reprinted with permission from [199]

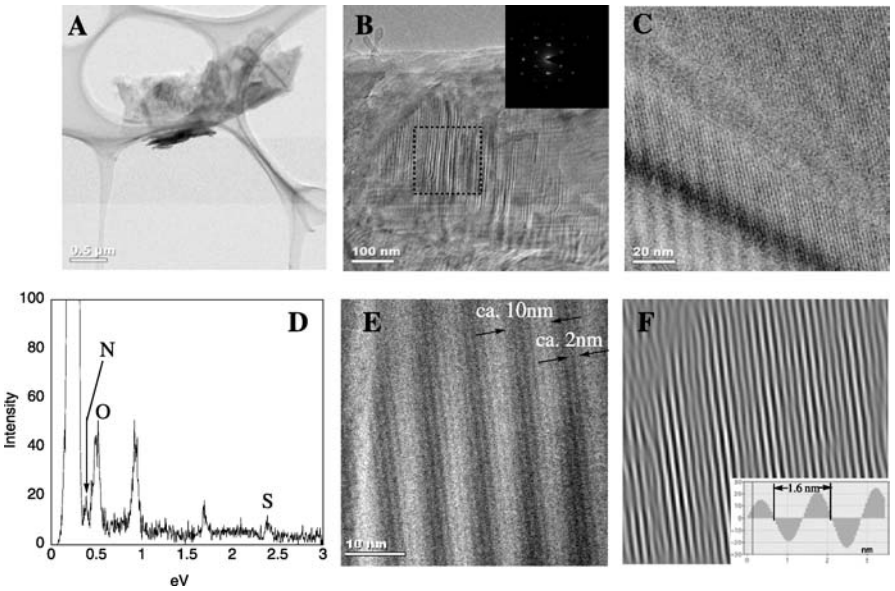

Fig. 40 TEM image of **A** Sheet-like structure (low magnification), **B**, **C** Magnified images of the thin layer (*inset*: electron diffraction pattern obtained from the sheet). **D** Elemental analysis of the sheet-like structure based on EDS. The spectrum was corrected from the *black-square* in (**B**). **E** Magnified TEM image of the sheet-like structure containing several thin layers. **F** Fourier translation image of (**D**) and extracted periodical patterns. Reprinted with permission from [199]

5 Conclusion and Outlook

Most polymer–polymer or polymer–molecule interactions, except those occurring in biological systems, have been considered to take place in a random fashion and to produce morphologically uninteresting polymer aggregates. In contrast, β-1,3-glucans can interact with polymer or molecular guests in a specific fashion and construct well-regulated one-dimensional superstructures: in the present system, we can predict how β-1,3-glucans wrap these guests. Furthermore, the wrapping occurs in an induced-fit manner, so that various functional nanocomposites can be created, reflecting the inherent functionalities of the entrapped guest material. These unique features of β-1,3-glucans mostly stem from the strong helix-forming nature and reversible interconversion between the single-stranded random coil and triple-stranded helix. It should be emphasized that the resultant composite can be applied to biomaterials due to the inherent bio-compatibility of β-1,3-glucans.

The clear wrapping mode allows us to utilize the composite as a one-dimensional building block for further molecular recognition events occurring on the composite surface: the selective modification of β-1,3-glucans

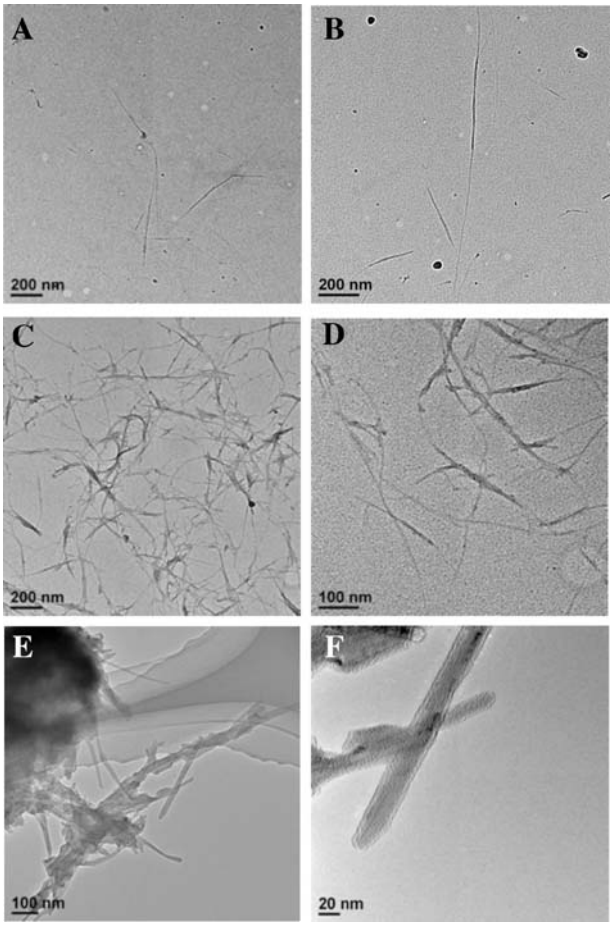

Fig. 41 TEM images of **A** SWNT/CUR-N^+ composite and **B** SWNT/CUR-SO_3^- composite. **C** Fibrous bundle structure containing a limited number of SWNTs ([SWNT/CUR-N^+]/[SWNT/CUR-SO_3^-]=1/5). **D** Magnified TEM image of (**C**). **E** Larger bundle structure ([SWNT/CUR-N^+]/[SWNT/CUR-SO_3^-]=1/3). **F** Magnified TEM image of (**E**) (*inset*: extracted periodical patterns obtained along the *red line*). Reprinted with permission from [199]

endows the composite with molecular recognition and self-organization abilities. We have demonstrated that the wrapping of the chemically modified SPG provides a novel strategy to create functional polymer composites with various molecular recognition tags in a supramolecular manner. Especially, the quantitative conversion of 6-OH groups of CUR to self-assembling groups allows the resultant composite to self-organize through the specific surface–surface interactions among the composites, where the composite acts as one-dimensional building blocks for creating the further hierarchical architecture.

Considering the serious difficulties involved in the creation of hierarchical architectures from synthetic polymers, the present system can open up new paths to accelerate development of the polymer assembly systems and can extend the frontier of polysaccharide-based functional nanomaterials.

References

1. Rao VSR, Qasba PK, Balaji PV, Chandrasekaran R (1998) Conformation of Carbohydrates. Harwood Academic Publishers, The Netherlands
2. Takahashi Y, Kumano T, Nishikawa S (2004) Macromolecules 37:6827
3. Rappenecker G, Zugenmaier P (1981) Carbohydr Res 89:11
4. Wu HCH, Sarko A (1978) Carbohydr Res 61:7
5. Frampton MJ, Anderson HL (2007) Angew Chem Int Edit 46:1028
6. Immel S, Lichtenthaler FW (2000) Starch/Stärke 52:1
7. Hinrichs W, Büttner G, Steifa M, Betzel C, Zabel V, Pfannemüller B, Saenger W (1987) Science 238:205
8. French A, Zobel HF (1967) Biopolymers 5:457
9. Hellert W, Chanzy H (1994) J Biol Macromol 16:207
10. Rundle RE, Edwards FC (1943) J Am Chem Soc 65:2200
11. Kim OK, Choi LS (1994) Langmuir 10:2842
12. Choi LS, Kim OK (1998) Macromolecules 31:9406
13. Sanji T, Kato N, Tanaka M (2005) Chem Lett 34:1144
14. Sanji T, Kato N, Kato M, Tanaka M (2005) Angew Chem Int Edit 44:7301
15. Sanji T, Kato N, Tanaka M (2006) Org Lett 8:235
16. Kida T, Minabe T, Okabe S, Akashi M (2007) Chem Commun p 1559
17. Kadokawa J, Kaneko Y, Yagaya H, Chiba K (2001) Chem Commun p 459
18. Star A, Steuerman DW, Heath JR, Stoddart JF (2002) Angew Chem Int Edit 41:2508
19. Kim OK, Je J, Baldwin JW, Kooi S, Phehrsson PE, Buckley LJ (2003) J Am Chem Soc 125:4426
20. Atwood JL, Davies JED, MacNichol DD, Vögtle F (1996) Comprehensive Supramolecular Chemistry, vol 3. Pergamon, Oxford
21. Harada A, Li J, Kamachi M (1992) Nature 356:325
22. Harada A, Li J, Kamachi M (1994) Nature 370:126
23. Wenz G, Keller B (1992) Angew Chem Int Edit 31:197
24. Rekharsky MV, Inoue Y (1998) Chem Rev 98:1875
25. Li G, McGown LB (1994) Science 264:249
26. Pistolis G, Malliaris A (1996) J Phys Chem 100:15562
27. Michels JJ, O'Connell MJ, Taylor PN, Wilson JS, Cacialli F, Anderson HL (2003) Chem Eur J 9:6167
28. Gattuso G, Menzer S, Nepogodiev SA, Stoddart JF, Williams DJ (1997) Angew Chem Int Edit 36:1451
29. Harada A (1997) Adv Polym Sci 133:141
30. Harada A, Li J, Kamachi M (1993) Nature 364:516
31. Harada A (2001) Acc Chem Res 34:456
32. Wenz G, Han BH, Müller A (2006) Chem Rev 106:782
33. Raymo FM, Stoddart JF (1999) Chem Rev 99:1643
34. Nepogodiev SA, Stoddart JF (1998) Chem Rev 98:1959

35. van den Boogaard M, Bonnet G, van't Hof P, Wang Y, Brochon C, van Hutten P, Hadziioannou G (2004) Chem Mater 16:4383
36. Shen X, Belletete M, Durocher G (1998) Chem Phys Lett 298:201
37. Lagrost C, Ching KIC, Lacroix JC, Aeiyach S, Jouini M, Lacaze PC, Tanguy J (1999) J Mater Chem 9:2351
38. Takashima Y, Oizumi Y, Sakamoto K, Miyauchi M, Kamitori S, Harada A (2004) Macromolecules 37:3962
39. Hapiot P, Lagrost C, Aeiyach S, Jouini M, Lacroix JC (2002) J Phys Chem B 106:3622
40. Lagrost C, Tanguy J, Aeiyach S, Lacroix JC, Jouini M, Chane-Ching KI, Lacaze PC (1999) J Electroanal Chem 476:1
41. Yamaguchi I, Kashiwagi K, Yamamoto T (2004) Macromol Rapid Commun 25:1163
42. Belosludov RV, Sato H, Farajian AA, Mizuseki H, Ichinoseki K, Kawazoe Y (2004) Japan J Appl Phys 42:2492
43. do Nascimento GM, da Silva JEP, de Torresi SIC, Santos PS, Temperini MLA (2002) Mol Cryst Liq Cryst 374:53
44. Yoshida K, Shimomura T, Ito K, Hayakawa R (1999) Langmuir 15:910
45. Akai T, Abe T, Shimomura T, Ito K (2001) Japan J Appl Phys 40:L1327
46. Shimomura T, Akai T, Abe T, Ito K (2002) J Chem Phys 116:1753
47. Shimomura T, Yoshida K, Ito K, Hayakawa R (2000) Polym Adv Technol 11:837
48. Okumura H, Kawaguchi Y, Harada A (2001) Macromolecules 34:6338
49. Okumura H, Kawaguchi Y, Harada A (2002) Macromol Rapid Commun 23:781
50. Okumura H, Kawaguchi Y, Harada A (2003) Macromolecules 36:6422
51. Yanaki T, Norisuye T, Fujita H (1980) Macromolecules 13:1462
52. van der Valk P, Marchant R, Wessels JGH (1977) Exp Mycol 1:69
53. Yanaki T, Ito W, Tabata K, Kojima T, Norisuye T, Takano N, Fujita H (1983) Biophys Chem 17:337
54. Bohn JA, BeMiller JN (1995) Carbohydr Polym 28:3
55. Sato T, Norisuye T, Fujita H (1981) Carbohydr Res 95:195
56. Stokke BT, Elgsaeter A, Brant DA, Kitamura S (1991) Macromolecules 24:6349
57. Sato T, Norisuye T, Fujita H (1983) Macromolecules 16:185
58. McIntire TM, Brant D (1998) J Am Chem Soc 120:6909
59. Bluhm TL, Deslandes Y, Marchessault RH (1982) Carbohydr Res 100:117
60. Harada T, Misaki A, Saito H (1968) Arch Biochem Biophys 124:292
61. Deslandes Y, Marchessault RH, Sarko A (1980) Macromolecules 13:1466
62. Frecer V, Rizzo R, Miertus S (2000) Biomacromolecules 1:91
63. Chuah CT, Sarko A, Deslandes Y, Marchessault RH (1983) Macromolecules 16:1375
64. Atkins EDT, Parker KD (1968) Nature 220:784
65. Marchessault RH, Deslandes Y, Ogawa K, Sundararajan PR (1977) Can J Chem 55:300
66. Norisuye T, Yanaki T, Fujita H (1980) J Polym Sci Polym Phys Edit 18:547
67. Kashiwagi Y, Norisuye T, Fujita H (1981) Macromolecules 14:1220
68. Sakurai K, Shinkai S (2000) J Am Chem Soc 122:4520
69. Sakurai K, Uezu K, Numata M, Hasegawa T, Li C, Kaneko K, Shinkai S (2005) Chem Commun p 4383
70. Iijima S (1991) Nature 354:56
71. Iijima S, Ichihashi T (1993) Nature 363:603
72. Bethune DS, Kiang CH, de Vries MS, Gorman G, Savoy R, Savoy J (1993) Nature 363:605
73. Zheng M, Jagota A, Semke ED, Diner BA, Mclean RS, Lustig SR, Tassi RER (2003) Nat Mater 2:338

74. Zheng M, Jagota A, Strano MS, Santos AP, Barone P, Chou SG, Diner BA, Dresselhaus MS, Mclean RS, Onoa GB, Samsonidze GG, Semke ED, Usrey M, Walls DJ (2003) Science 302:1545
75. Nakashima N, Okuzono S, Murakami H, Nakai T, Yoshikawa K (2003) Chem Lett 32:456
76. Takahashi T, Tsunoda K, Yajima H, Ishii T (2002) Chem Lett 31:690
77. Pantarotto D, Partidos CD, Graff R, Hoebeke J, Briand JP, Prato M, Bianco A (2003) J Am Chem Soc 125:6160
78. Dieckmann GR, Dalton AB, Johnson PA, Razal J, Chen J, Giordano GM, Munoz E, Musselman IH, Baughaman RH, Draper RK (2003) J Am Chem Soc 125:1770
79. Zorbas V, Ortiz-Acevedo A, Dalton AB, Yoshida MM, Dieckmann GR, Draper RK, Baughman RH, Yacaman MJ, Musselman IM (2004) J Am Chem Soc 126:7222
80. Sano M, Kamino A, Okamura J, Shinkai S (2001) Science 293:1299
81. Ziegler KJ, Gu Z, Peng H, Flor EL, Hauge RH, Smalley RE (2005) J Am Chem Soc 127:1541
82. Liu J, Rinzler AG, Dai HJ, Hafner JH, Bradley RK, Boul PJ, Lu A, Iverson T, Shelimov K, Huffman CB, Rodriguez-Macias F, Shon YS, Lee TR, Colbert DT, Smalley RE (1998) Science 280:1253
83. Zhang J, Zou H, Qing Q, Yang Y, Li Q, Liu Z, Guo X, Du Z (2003) J Phys Chem B 107:3712
84. Numata M, Asai M, Kaneko K, Hasegawa T, Fujita N, Kitada Y, Sakurai K, Shinkai S (2004) Chem Lett 33:232
85. Kimura T, Koumoto K, Sakurai K, Shinkai S (2000) Chem Lett 29:1242
86. Numata M, Asai M, Kaneko K, Bae AH, Hasegawa T, Sakurai K, Shinkai S (2005) J Am Chem Soc 127:5875
87. Coleman JN, Ferreira MS (2004) Appl Phys Lett 84:798
88. Midgley PA, Thomas JM, Weyland M, Johnson BFG (2001) Chem Commun p 907
89. Madalia O, Weber I, Frangakis AS, Gerisch G, Baumeister W (2002) Science 298:1209
90. Thomas JM, Midgley PA (2004) Chem Commun p 1253
91. Kermer JR, Mastronarde DN, McIntosh JR (1996) J Struct Biol 116:71
92. Frank J (1996) Three-dimensional Electron Microscopy of Macromolecular Assemblies. Academic Press, San Diego
93. Jinnai H, Nishikawa Y, Spantak RJ, Smith SD, Agard DA, Hashimoto T (2000) Phys Rev Lett 84:518
94. MacDiamid AG, Chiang JC, Halpern M, Huang WS, Mu SL, Somasiri NLD, Wu W, Yaniger SI (1985) Mol Cryst Liq Cryst 121:173
95. MacDiamid AG, Chiang JC, Richter AF, Epstein AJ (1987) Synth Met 18:285
96. Lu FL, Wudl F, Nowak M, Heeger AJ (1986) J Am Chem Soc 108:8311
97. Numata M, Hasegawa T, Fujisawa T, Sakurai K, Shinkai S (2004) Org Lett 6:4447
98. Buey J, Swager TM (2000) Angew Chem Int Edit 39:608
99. Sauvage JP, Kern JM, Bidan G, Divisia-Blohorn B, Vidal PL (2002) New J Chem 26:1287
100. Martin RE, Diederich F (1999) Angew Chem Int Edit 38:1350
101. Hecht S, Frechet JMJ (2001) Angew Chem Int Edit 40:74
102. Sato T, Jiang DL, Aida T (1999) J Am Chem Soc 121:10658
103. Li C, Numata M, Bae AH, Sakurai K, Shinkai S (2005) J Am Chem Soc 127:4548
104. Langeveld-Voss BMW, Janssen RAJ, Christiaans MPT, Meskers SCJ, Dekkers HPJM, Meijer EM (1996) J Am Chem Soc 118:4908
105. Goto H, Okamoto Y, Yashima E (2002) Chem Eur J 8:4027
106. Kim J, McQuade DT, McHugh SK, Swager TM (2000) Angew Chem Int Edit 39:3868

107. Tan C, Atas E, Müller JG, Pinto MR, Kleiman VD, Schanze KS (2004) J Am Chem Soc 126:13685
108. Zahn S, Swager TM (2002) Angew Chem Int Edit 41:4226
109. DiCesare N, Pinto MR, Schanze KS, Lakowica JR (2002) Langmuir 18:7785
110. Kumaraswamy S, Bergstedt T, Shi X, Rininsland F, Kushon S, Xia W, Ley K, Achyuthan K, McBranch D, Whitten D (2004) Proc Natl Acad Sci USA 101:7511
111. Pinto MR, Schanze KS (2004) Proc Natl Acad Sci USA 101:7505
112. Fan C, Plaxco KW, Heeger AJ (2002) J Am Chem Soc 124:5642
113. Wosnick JH, Mello CM, Swager TM (2005) J Am Chem Soc 127:3400
114. Numata M, Fujisawa T, Li C, Haraguchi S, Ikeda M, Sakura K, Shinkai S (2007) Supramol Chem 19:107
115. Ichino Y, Minami N, Yatabe T, Obata K, Kira M (2001) J Phys Chem 105:4111
116. Nakashima H, Fujiki M, Koe JR, Motonaga M (2001) J Am Chem Soc 123:1963
117. Peng W, Motonaga M, Koe JR (2004) J Am Chem Soc 126:13822
118. Haraguchi S, Hasegawa T, Numata M, Fujiki M, Uezu K, Sakurai K, Shinkai S (2005) Org Lett 7:5605
119. Fujiki M (1994) J Am Chem Soc 116:6017
120. Würthner F, Yao S, Beginn U (2003) Angew Chem Int Edit 42:3247
121. Parins LJ, Thalacker C, Würthner F, Timmerman P, Reinhoudt DN (2001) Proc Natl Acad Sci USA 98:10042
122. Jones RM, Lu L, Helgeson R, Bergstedt TS, McBranch DW, Whitten DG (2001) Proc Natl Acad Sci USA 98:14769
123. Yao S, Beginn U, Gress T, Lysetska M, Würthner F (2004) J Am Chem Soc 126:8336
124. Morikawa M, Yoshihara M, Endo T, Kimizuka N (2005) J Am Chem Soc 127:1358
125. Hannah KC, Armitage BA (2004) Acc Chem Res 37:845
126. Heuer WB, Kim OK (1998) Chem Commun p 2649
127. Clays K, Olbrechts G, Munters T, Persoons A, Kim OK, Choi LS (1998) Chem Phys Lett 293:337
128. Kim OK, Je J, Jernigan G, Buckley L, Whitte D (2006) J Am Chem Soc 128:510
129. Kashida H, Asanuma H, Komiyama M (2006) Chem Commun p 2768
130. Kashida H, Asanuma H, Komiyama M (2004) Angew Chem Int Edit 43:6522
131. Kool ET (2002) Acc Chem Res 35:936
132. Onouchi H, Miyagawa T, Morino K, Yashima E (2006) Angew Chem Int Edit 45:2381
133. Li C, Numata M, Takeuchi M, Shinkai S (2005) Angew Chem Int Edit 44:6371
134. Endo M, Wang H, Fujitsuka M, Majima T (2006) Chem Eur J 12:3735
135. Koti ASR, Periasamy N (2003) Chem Mater 15:369
136. Wang M, Silva GL, Armitage BA (2000) J Am Chem Soc 122:9977
137. Renikuntala BR, Armitage BA (2005) Langmuir 21:5362
138. Garoff RA, Litzinger EA, Connor RE, Fishman I, Armitage BA (2002) Langmuir 18:6330
139. Aoki K, Nakagawa M, Ichimura K (2000) J Am Chem Soc 122:10997
140. Nakagawa M, Ishii D, Aoki K, Seki T, Iyoda T (2005) Adv Mater 17:200
141. Numata M, Tamesue S, Fujisawa T, Haraguchi S, Hasegawa T, Bae AH, Li C, Sakurai K, Shinkai S (2006) Org Lett 8:5533
142. Hasegawa T, Fujisawa T, Numata M, Li C, Bae AH, Haraguchi S, Sakurai K, Shinkai S (2005) Chem Lett 34:1118
143. Morigaki K, Baumgart T, Jonas U, Offenhausser A, Knoll W (2002) Langmuir 18:4082
144. Niwa M, Shibahara S, Higashi N (2000) J Mater Chem 10:2647
145. Menzel H, Mowery MD, Cai M, Evans CE (1999) Adv Mater 11:131
146. Tajima K, Aida T (2000) Chem Commun p 2399

147. Ying JY, Mehnert CP, Wong MS (1999) Angew Chem Int Edit 38:56
148. Uemura T, Horiike S, Kitagawa S (2006) Chem Asian J 1:36
149. Hasegawa T, Haraguchi S, Numata M, Fujisawa T, Li C, Kaneko K, Sakurai K, Shinkai S (2005) Chem Lett 34:40
150. Hasegawa T, Haraguchi S, Numata M, Li C, Bae AH, Fujisawa T, Kaneko K, Sakurai K, Shinkai S (2005) Org Biomol Chem 3:4321
151. Wenz G, Müller MA, Schmidt M, Wegner G (1984) Macromolecules 17:837
152. Shirai E, Urai Y, Itoh K (1998) J Phys Chem B 102:3765
153. Soler-lllia GJ de AA, Sanchez C, Lebeau B, Patarin J (2002) Chem Rev 102:4093
154. Davis SA, Breulmann M, Rhodes KH, Zhang B, Mann S (2001) Chem Mater 13:3218
155. van Bommel KJC, Friggeri A, Shinkai S (2003) Angew Chem Int Edit 42:980
156. Huang J, Kunitake T (2003), J Am Chem Soc 125:11834
157. Ichinose I, Hashimoto Y, Kunitake T (2004) Chem Lett 33:656
158. Antonietti M, Breulmann M, Göltner CG, Cölfen H, Wong KK, Walsh D, Mann S (1998) Chem Eur J 4:2493
159. Qi L, Cölfen H, Antonietti M, Li M, Hopwood JD, Ashley AJ, Mann S (2001) Chem Eur J 7:3526
160. Numata M, Li C, Bae AH, Kaneko K, Sakurai K, Shinkai S (2005) Chem Commun p 4655
161. Groenendaal L, Jonas F, Freitag D, Pielartzik H, Reynolds JR (2000) Adv Mater 12:481
162. Li C, Imae T (2004) Macromolecules 37:2411
163. Li C, Hatano T, Takeuchi M, Shinkai S (2004) Tetrahedron 60:8037
164. Pringsheim E, Terpetschnig E, Piletsky SA, Wolfbeis OS (1999) Adv Mater 11:865
165. Kim BH, Kim MS, Park KT, Lee JK, Park DH, Joo J, Yu SG, Lee SH (2003) Appl Phys Lett 83:539
166. Hulvat JF, Stupp SI (2004) Adv Mater 16:589
167. Goto H, Akagi K (2004) Macromol Rapid Commun 25:1482
168. Han MG, Armes SP (2003) Langmuir 19:4523
169. Han MG, Foulger SH (2004) Adv Mater 16:231
170. Li C, Numata M, Hasegawa T, Fujisawa T, Haracuchi S, Sakurai K, Shinkai S (2005) Chem Lett 34:1532
171. Tour JM (1996) Chem Rev 96:537
172. Roncali J (1997) Chem Rev 97:173
173. McQuade DT, Pullen AE, Swager TM (2000) Chem Rev 100:2537
174. Katz E, Willner I (2004) Angew Chem Int Edit 43:6042
175. Devries GA, Brunnbauer M, Hu Y, Jackson AM, Long B, Neltner BT, Uzun O, Wunsch BH, Stellacci F (2007) Science 315:358
176. Bae AH, Numata M, Hasegawa T, Li C, Kaneko K, Sakurai K, Shinkai S (2005) Angew Chem Int Edit 44:2030
177. Bae AH, Numata M, Yamada S, Shinkai S (2007) New J Chem 31:618
178. Demleitner S, Kraus J, Franz G (1992) Carbohydr Res 226:239
179. Gao Y, Katsuraya K, Kaneko Y, Mimura T, Nakashima H, Uryu T (1999) Macromolecules 32:8319
180. Katsuraya K, Nakashima H, Yamamoto N, Uryu T (1999) Carbohydr Res 315:234
181. Yoshida T, Yasuda Y, Mimura T, Kaneko Y, Nakashima H, Yamamoto N, Uryu T (1995) Carbohydr Res 276:425
182. Katsuraya K, Ikushima N, Takahashi N, Shoji T, Nakashima H, Yamamoto N, Yoshida T, Uryu T (1994) Carbohydr Res 260:51
183. Na K, Park KH, Kim SW, Bae YH (2000) J Control Release 69:225
184. Koumoto K, Umeda M, Numata M, Matsumoto T, Sakurai K, Kunitake T, Shinkai S (2004) Carbohydr Res 339:161

185. Hasegawa T, Umeda M, Numata M, Fujisawa T, Haraguchi S, Sakurai K, Shinkai S (2006) Chem Lett 35:82
186. Hasegawa T, Umeda M, Numata M, Li C, Bae AH, Fujisawa T, Haraguchi S, Sakurai K, Shinkai S (2006) Carbohydr Res 341:35
187. Numata M, Matsumoto T, Umeda M, Koumoto K, Sakurai K, Shinkai S (2003) Bioorg Chem 163:171
188. Hasagawa T, Umeda M, Matsumoto T, Numata M, Mizu M, Koumoto K, Sakurai K, Shinkai S (2004) Chem Commun p 382
189. Hasegawa T, Fujisawa T, Numata M, Matsumoto T, Umeda M, Karinaga R, Mizu M, Koumoto K, Kimura T, Okumura S, Sakurai K, Shinkai S (2004) Org Biomol Chem 2:3091
190. Hasegawa T, Fujisawa T, Numata M, Umeda M, MatsumotoT, Kimura T, Okumura S, Sakurai K, Shinkai S (2004) Chem Commun p 2150
191. Hasegawa T, Fujisawa T, Haraguchi S, Numata M, Karinaga R, Kimura T, Okumura S, Sakurai K, Shinkai S (2005) Bioorg Med Chem Lett 15:327
192. Ikeda M, Hasegawa T, Numata M, Sugikawa K, Sakurai K, Fujiki M, Shinkai S (2007) J Am Chem Soc 129:3979
193. Ikeda M, Minari J, Shimada N, Numata M, Sakurai K, Shinkai S (2007) Org Biomol Chem 5:2219
194. Ikeda M, Haraguchi S, Numata M, Shinkai S (2007) Chem Asian J 2:1290
195. Lehn JM (1995) Supramoleculer Chemistry. VCH, New York
196. Kubo Y, Kitada Y, Wakabayashi R, Kishida T, Ayabe M, Kaneko K, Takeuchi M, Shinkai S (2006) Angew Chem Int Edit 45:1548
197. Ikeda M, Furusho Y, Okoshi K, Tanahara S, Maeda K, Nishino S, Mori T, Yashima E (2006) Angew Chem Int Edit 45:6491
198. Ewert KK, Evans HM, Zidovska A, Bouxsein NF, Ahmad A, Safinya CR (2006) J Am Chem Soc 128:3998
199. Numata M, Sugikawa K, Kaneko K, Shinkai S (2008) Chem Eur J 14:2398